energies

MDPI

Review

A Review on Modular Converter Topologies Based on WBG Semiconductor Devices in Wind Energy Conversion Systems

Abdulkarim Athwer and Ahmed Darwish *

School of Engineering, Lancaster University, Lancaster LA1 4YW, UK; a.athwer@lancaster.ac.uk
* Correspondence: a.badawy@lancaster.ac.uk

Abstract: This paper presents a comprehensive review on the employment of wide bandgap (WBG) semiconductor power devices in wind energy conversion systems (WECSs). Silicon-carbide- (SiC) and gallium-nitride (GaN)-based power devices are highlighted and studied in this review, focusing on their application in the wind energy system. This is due to their premium characteristics such as the operation at high switching frequency, which can reduce the switching losses, and the capability to operate at high temperatures compared with silicon (Si)-based devices. These advantages promote the replacement of the conventional Si-based devices with the WBG semiconductor devices in the new modular converter topologies due to the persistent demand for a more-efficient power converter topology with lower losses and smaller sizes. The main objective of this paper was to provide a comprehensive overview of the WBG power devices commercially available on the market and employed in the modular converter topologies for renewable energy systems. The paper also provides a comparison between the WBG power technologies and the traditional ones based on the Si devices. The paper starts from the conventional modular power converter topology circuits, and then, it discusses the opportunities for integrating the SiC and WBG devices in the modular power converters to improve and enhance the system's performance.

Keywords: wind energy systems; power electronic converters; wide bandgap devices; modular converters; modular multilevel converters; multicarrier PWM techniques

Citation: Athwer, A.; Darwish, A. A Review on Modular Converter Topologies Based on WBG Semiconductor Devices in Wind Energy Conversion Systems. *Energies* **2023**, *16*, x. https://doi.org/10.3390/xxxxx

Academic Editor: Frede Blaabjerg

Received: 1 June 2023
Revised: 6 July 2023
Accepted: 10 July 2023
Published: date

1. Introduction

During the last two decades, the demand for sustainable energy systems based on renewable energy resources (RESs) has been rapidly increasing. Wind energy is one of the fastest-growing and most-promising RESs due to its clean and sustainable properties [1]. It has been recognised as an effective way to mitigate the impacts of climate change and supply sustainable energy [2]. The installed wind capacity has increased globally from 181 GW in 2010 to 733 GW in 2020, which covered about 5.9% of the global electricity demand in the same year [3,4]. In 2021, the global installed capacity of wind power increased by 93.6 GW, and the progressive capacity reached 837 GW with an increase of 12% over 2020. According to the Global Wind Workforce Outlook 2022–2026 issued by the Global Wind Organization, the worldwide wind fleet will be approximately 1394 GW by the end of 2026 [5,6], which means that wind energy is being developed in-depth around the world [7]. However, the optimum integration of wind energy systems into the main grid remains a challenge to ensure the grid's stability and the reliability of the system when the variable wind resource is connected, especially in the case of grid disruptions [8]. Since the main aim of transfer power systems is to supply consumers with the required electricity at any given time at a reasonable cost, it is important to achieve an efficient and reliable power conversion system [9].

The power electronic converters are designed to continuously draw electrical energy from the source to the load, chop it into finite discrete packets using power switches, and

reshape these energy packets using passive components, which are usually formed of a combination of inductors and capacitors before feeding the energy to the load [10]. In this way, the power converters use semiconductor switching devices to control and convert electrical power flow from one form to another to meet a specific need [11]. The revolution in semiconductor devices has played a significant role in several power applications including energy conversion systems for RESs. It is well known that about 70% of electric energy is converted by power electronics devices before it reaches the consumers [12].

Alongside the development of power devices, modular converter topologies have been extensively studied since the 1960s. Several modular converter topologies have been published and presented such as the neutral point clamped (NPC) converter [13], the flying capacitor (FC) converter topology [14], and cascaded H-bridge converters (CHBs) [15]. Other systems such as T-type converters, active-NPC (ANPC) converters [16], and modular multilevel converters (MMCs) were proposed later [17]. These modular converters have been successfully implemented in the power transfer of several RESs, especially wind energy conversion systems (WECSs). The MMC topology has specifically gained a wide acceptance and become the preferred choice for wind energy conversion systems due to its main features such as the easy scalability of the voltage and current, the capability of operation as either a rectifier or an inverter, and its fault ride-through (FTR) features for some selected cells. However, one of the common drawbacks of the modular converters in general and the MMCs specifically is their necessity for a large number of switching devices and the associated gate drive circuits and protection circuits, which lead to increased power losses, increased volume, and the complexity of the control strategies [18,19]. To improve the performance and operation of the MMC topology or other multilevel converter models, it is always better to simplify the system by reducing the number of power semiconductors, capacitors, and inductors while achieving the same voltage levels and output converter performance [20,21].

The design of these conversion systems requires the essential hardware, the control system, semiconductor switches, passive components such as capacitors, inductors, and transformers, thermal management systems, packaging, protection devices, DC and AC disconnects, and enclosures. The hardware is collectively referred to as a power conversion system (PCS) [22]. Power electronic converters are constantly moving toward and seeking higher efficiency, higher power density, and more-integrated systems. In this journey, the junction-gate field-effect transistor (JFETs) and the bipolar junction transistors (BJTs) have been replaced with metal–oxide semiconductor field effect transistors (MOSFETs) and insulated gate bipolar transistors (IGBTs) based on silicon (Si), which are the most-common transistors currently [23]. Then, the power semiconductor devices based on Si have developed and matured over the last five decades and greatly improved the associated energy transmission systems. In applications below 600 V, Si MOSFETs based on the trench gate structure dominate the market, whereas Si super junction MOSFETs and Si IGBTs based on the field stop and injection enhancement concepts dominate the market from 600 V to 6.5 kV [24]. However, it seems that Si power devices are approaching their performance limitations, and there is no expected further optimisation of these devices. For example, the maximum temperature limit for most Si device junctions is 150 °C, which is a major concern, especially in high-power applications. Therefore, further development and improvements of power electronic devices are necessary for more-reliable solutions of power generation, energy storage, and power conversion systems [25].

In this context, the demand for power converter designs with higher efficiency and increased power density is great. Accordingly, the high-performance new wide bandgap (WBG) power semiconductor devices such as silicon carbide (SiC) and gallium nitride (GaN) devices are expected to replace the traditional Si devices in the near future [26,27]. Power converters based on WBG semiconductors offer many advantages over the traditional Si converters as they can withstand high frequencies and temperatures and reduce the power losses significantly [28]. Thus, the employment of WBG power devices in the

MMC topology appears to provide new opportunities for converter design to harness the increased performance of the power converter model in terms of higher efficiency, higher power density, and reduced power losses and volume [29]. Therefore, using WBG devices in MMCs can bring low switching loss with the mitigation of the negative side-effects of dv/dt and solve the EMI issues [30,31]. Increasing the switching frequency of the semiconductor devices will lead to a massive reduction in the converters' size, volume, and weight. Research efforts are being conducted presently in the field of the manufacturing and fabrication of new WBG devices that can withstand higher voltages (>1.2 kV). If these efforts are successful, the WBG devices will either replace the Si-based converters completely or, at least, new hybrid converters incorporating the new and the old devices will arise [32].

This paper focused on the idea of using WBG devices in the context of MMCs for wind energy systems with the aim to review the SiC- and GaN-based power systems. Following this section, a further introduction regarding the use of Si devices for wind power converters is given in Section 2, highlighting the importance of semiconductor devices in the design of MMCs. Section 3 presents the different modulation techniques for MMCs and the most-common associated control schemes. The section explains the effect of the modulation and control schemes on the selection of the power devices and vice versa. Section 4 presents the WBG semiconductor devices' technological development, focusing on SiC and GaN, as well as the hybrid combination with Si-based devices. Section 5 presents a comparison between the Si and the WBG materials, their prices, and their performances. The summary and final conclusions are presented in Section 6.

2. The Role of Semiconductor Power Devices in WECSs

The main objectives for the WECS design process are to increase the system's efficiency and to reduce its cost [33]. Generally, the power electronic converters of the energy conversion stage play a significant role for either low- or high-voltage DC applications. Due to their intermittent nature, wind and solar RESs cannot be directly integrated into the electric grid according to the daily and seasonal fluctuations which affect the harvested energy. Therefore, the main role of power converters is to employ the semiconductor power devices to mitigate this problem. Wind turbines are usually connected to the grid through power electronic converters, as shown in Figure 1, to smooth out the power fluctuation injected into the grid from these energy resources [34,35].

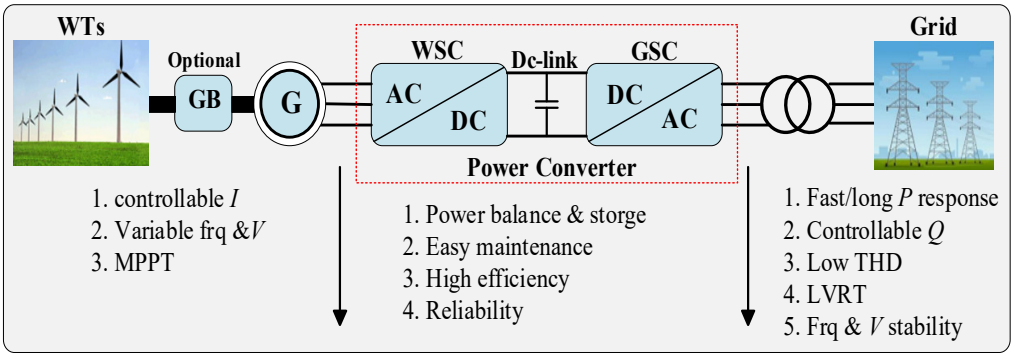

Figure 1. The system of integrating wind energy into the grid [33].

Most importantly, the power converter should be designed to extract the maximum available power from the wind turbine (WT) generator during various operating conditions and meet the network's integration requirements and codes at the same time [36,37]. However, the fixed-speed wind turbine (FSWT) still forms a considerable part of wind power installations as it represents around 20% of the global WT capacity [38]. The remaining portion of the WECS installation employs variable-speed architectures such as doubly fed induction generators (DFIGs) or permanent magnet synchronous generators

(PMSGs), which are connected to the AC grid through advanced front-end AC/DC rectifiers, which control the DC link voltage and, hence, regulate the extracted energy from the wind. Another back-end DC/AC inverter is employed to regulate the active and reactive power injected into the grid. The DC link capacitor is placed between the converters to provide the element of temporary power storage for the transferred power between the generator and the network [35].

Multilevel converters (MLCs) play an essential role in medium- and high-power applications and, hence, have been the research focus for several years. The main purposes of the MLCs are to share the total high voltage of the WECS, then control the transferred power when the WECS is connected to the grid, and finally, deliver smooth energy to the consumers at the lowest-possible power losses and cost [39]. Various MLCs have been proposed and investigated in the literature in the context of grid-connected large-scale WTs. One of the most-important MLCs is the modular multilevel converter (MMC) topology, which introduces full modularity and easy extendibility to meet any voltage/power level requirements. Since it was introduced in 2003 [40], the MMC has provided a better wind energy conversion operation with high performance compared to the other traditional topologies and, hence, has drawn considerable attention in both academia and industry [41]. The next subsections will review the different configurations of the MMC.

2.1. Modular Multilevel Converter

In 2003, the first MMC topology was proposed for high-voltage direct current (HVDC) applications. Since then, the MMC topology has gained a wide acceptance in WECSs [39]. Recently, more research efforts have been conducted by various research teams to improve the operation of the MMC and generate several improved MMC versions [42–46]. By examining these versions, it can be seen that most of these converters have been inspired by the basic configuration of the M2C technology, which was proposed earlier in 1981 [47]. This M2C topology employs a submodule ''SM'', which is simply a half-bridge with a capacitor and, hence, forms the basic circuit configuration of the three-phase MMC concept, as shown in Figure 2. Basically, the MMC model is composed of three legs to shape the output voltages. The legs are connected in parallel across the DC source, where each one is divided into two arms (upper and lower arm). The two arms are connected via buffer inductors L_{arm}, which are used to handle the voltage differences between the upper and lower arms [48] and, hence, limit the circulating current and maintain the system during faults and short-circuits. Each arm is composed of a series connection of N identical half- or full-bridge submodules (SMs), where each SM consists of several semiconductor switches connected with a blocking capacitor [49,50].

The three legs of the MMC correspond to the three phases (A, B, and C), and each leg contains two arms. The main advantage of connecting N_{arm} SMs in each arm leg is to build up the voltage output where the SMs are controlled individually, either inserted into or bypassing the capacitor. The flow of the voltage through the two-arm SMs in each phase configuration is required to achieve the desired power exchange between the DC and the AC terminals and to handle the internal energy balance of the MMC [41,51].

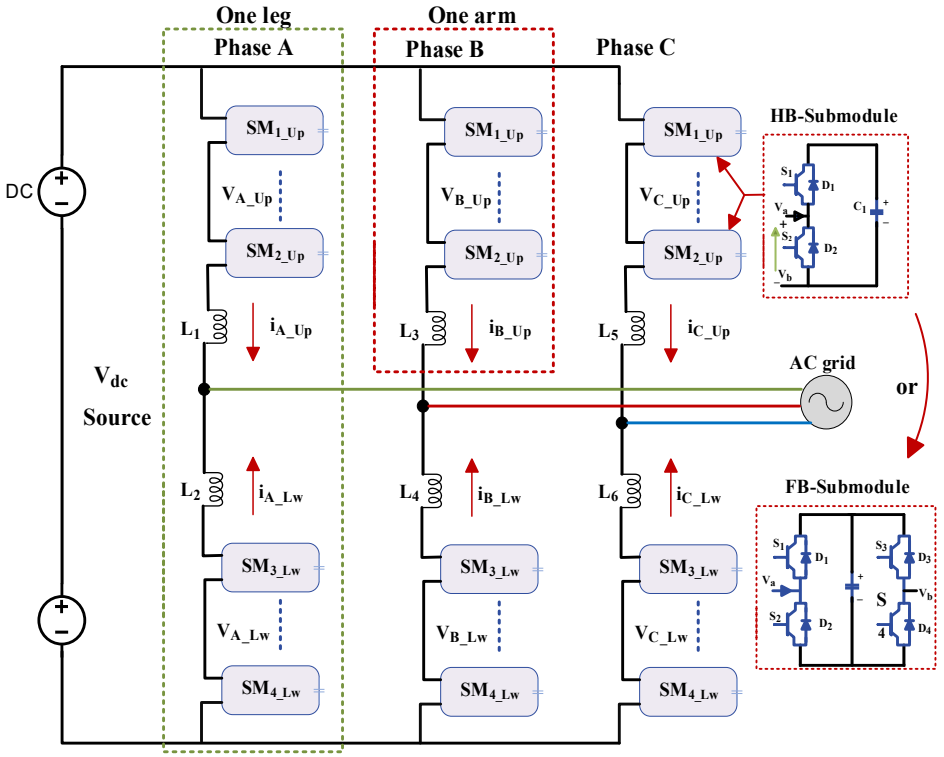

Figure 2. The configuration of three-phase MMC topology. Copied with permission from [48].

2.2. MMC SM Structure Based on Si Devices

The SM structure is the fundamental part of the MMC topology to obtain the required output voltage [52]. Semiconductor devices such as Si IGBT and MOSFET power switches are playing an important role in the design of SM systems for controlling the flow of the voltage and current and converting them into a form that is suitable for user loads. In the last 20 years, several SM circuits have been developed and successfully implemented in power converters, among which the half-bridge and full-bridge SM topologies are recognised as the most-popular cell structures for MMC HVDC applications [53]. However, the voltage balancing of SM capacitors remains a concern in the design of the MMC topology, and many efforts have been made to resolve this part [54,55]. The MMC SMs can generate either unipolar or bipolar output voltage pulses. The unipolar technology can produce positive and zero voltage levels, while the bipolar one is able to produce positive, negative, and zero voltage levels [49]. A brief description in terms of output voltage and the number of components per SM circuit will be presented in the next subsections.

2.2.1. Unipolar SMs

The simple structures of unipolar SM technologies have the capability of generating a zero or positive level at their output voltage terminals (V_{SM}). On the other hand, these types of SMs suffer from the lack of DC-fault-clearing capabilities within the arm, which require further protection [56]. Examples of these structures are as follows:

- Half-bridge SM (HBSM): The most-common type of unipolar circuit due to its simple structure and cost. Figure 3a shows the HBSM's structure, which mainly consists of two IGBT switches (S_1, S_2) connected with a single capacitor C and operating in a complementary manner to produce two voltage levels at the output side (0, V_C). The cell of the HBSM has a lower power loss compared to other topologies. However, it has a clear shortcoming against DC faults [57].
- Single-clamped submodule (SCSM): This type of circuit was introduced to control the DC fault current problem without a significant increase in power loss and cost, as this kind is typically used in hybrid MMC topologies. Compared to HBSMs, the

modified SM circuit has one further IGBT switch connected along with an additional diode D_4 connected with the split DC capacitor C_1 acting to provide the path of the current during DC faults. Figure 3b shows the SCSM structure, which can produce two output voltage levels (0 or V_C), whereas during normal operating conditions, the switch S_3 remains on constantly. The cell voltage is inserted against the fault currents because only two of the four diodes act at any instant. The main advantage of SCSMs is the ability of fault handling with only three switches, which results in lower power losses compared with other structures [53,58].

- Half-voltage clamped submodule (HVCSM): Its structure is shown in Figure 3c, where three IGBT switches are connected in series with two capacitors. An additional protective diode D_4 is connected instead of the IGBT switch. The HVCSM uses the voltages of the submodule capacitors to eliminate the freewheeling impact of diodes actively and achieve fast fault clearance and converter restart. The switch S_3 is placed in the opposite direction to the S_1, S_2 switches to enable stopping the rectifier mode by turning the switch S_3 off [59]. The main disadvantage of this cell structure is the difficulty of balancing the capacitors' voltage when the arm current is negative. Furthermore, it suffers from higher conduction losses compared to the HBSM [56].
- Asymmetrical unipolar full-bridge submodule (AUFBSM): This consists of three IGBT switches (S_1, S_2, and S_3), four diodes, and two capacitors, as shown in Figure 3d. This modified cell SM is suitable for hybrid MMC-HVDC applications and has been introduced to overcome the DC fault current problems. In normal operating systems, S_3 is always *on*, while in the case of a DC fault, all switches must be *off*, and the current will flow through the complementary capacitors (C_1, C_2), increasing their voltages. Asymmetric UFBSMs have the ability to block DC fault currents with less power loss compared to other cells [60].
- Series switch submodule (SSSM) topology: The SSSM is an extension of the HBSM topology. Figure 3e shows the basic structure of this cell, which consists of two power switches connected in parallel with a capacitor, and an additional IGBT switch with a low voltage rating is required to be connected to the conventional HBSMs. It can be used for HVDC transmission systems, where the HVDC system is capable of blocking the fault current under DC-cable short-circuit conditions based on this model. Compared to the FBSM and hybrid SM types, the cost of the SSSM-MMC type is about 59.4% and 79.2%, respectively. Additionally, the power loss of the semiconductor devices of the SSSM is lower than that of the FBSM and comparable to the hybrid SM type [61].
- Unipolar full-bridge submodel (UFBSM): The structure of this SM is based on the full-bridge SM, in which the IGBT S_3 and its parallel diode are replaced by the diode D_3, as shown in Figure 3f. During normal operation, the SM can generate two voltage levels by controlling switches S_1 and S_2; the SM is inserted/bypassed, while the switch S4 is always on. The UFBSM can block DC fault currents and provide DC-fault-handling capability. However, the conduction losses of the S_4 contact switch are greater than those of any of the other switches [62].
- Stacked switched capacitor (SSCSM): This is illustrated in Figure 3g. This topology is an enhanced unipolar SSCSM comprising six power switches and three capacitors (C_1, C_2, and C_3). The physical volume of all capacitors in the SSCSM can be up to 60%. The performance of the SSCSM-based MMC model was found to be similar to that of the HB-based system. However, one of the main drawbacks of the SSCSM structure is the increased number of power devices, which leads to an increase in the power losses of between 7% and 15% during rated power operation [63].

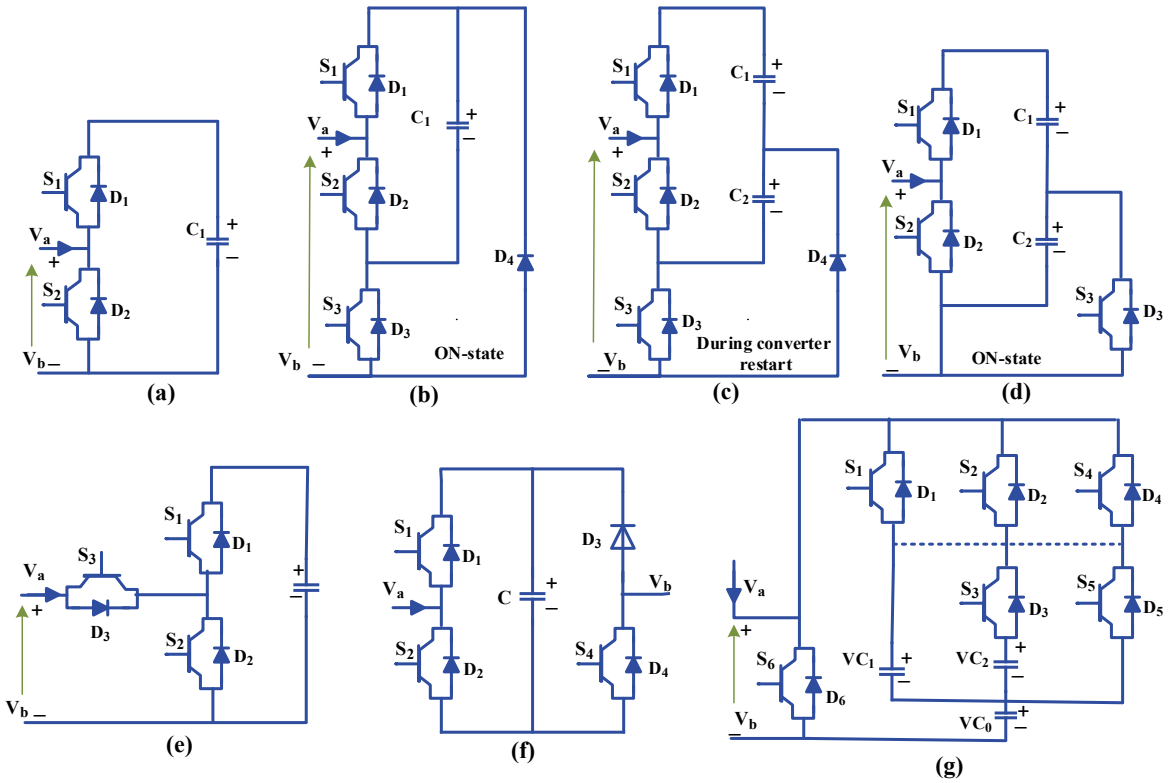

Figure 3. Unipolar SM structures. (**a**) HBSM, (**b**) SCSM, (**c**) HVCSM, (**d**) AUFBSM, (**e**) *SSSM*, (**f**) *UFBSM*, and (**g**) *SSCSM* [53].

2.2.2. Bipolar SMs

Bipolar SM can produce three voltage levels across their output terminals (0, $+V_C$, and $-V_C$) with the ability to block and eliminate the DC faults [48,56]. Compared to the unipolar cells, the bipolar ones will usually have more semiconductor devices, which may increase the total power losses. Examples of these structures are as follows:

- Full-bridge circuit or bridge cell (FBSM): This cell is widely used in multilevel converter topologies. Figure 4a shows the FBSM topology, which consists of four IGBT switches (S_1, S_2, S_3, and S_4) connected with a single capacitor C. This type of cell structure can supply both positive and negative voltages at its output terminals ($+V_C$ and $-V_C$), where the output voltage is either equal to the voltage of its capacitor V_C (switched on/inserted state) or zero (switched off/bypassed state), which depends on the switch states of the switches. The main feature of this SM is the capability of DC fault blocking and its suitability for connection with either AC or DC systems. However, the increased number of semiconductor switches in the structure of the FBSM may cause additional power losses and increase the cost of the total MMC compared to the HBSM-based MMC [64].
- Diode clamped submodule (DCSM): This topology is also known as a neutral pinned point switch (NPPS) [13]. DCSM structures have been widely used in industrial medium-voltage applications. As shown in Figure 4b, three levels can be generated by two series cells in the upper and lower arms, which are connected to two bulk capacitors (C_1, C_2). The employed NPC technique has good output voltage quality as the cell can produce three output voltage levels (0, $V_{dc/2}$, and $-V_{dc/2}$). On the downside, this SM topology suffers from the complex capacitor voltage balancing, high power losses, and hence, low efficiency compared to other bipolar cells [65].
- Flying capacitor submodule (FCSM): This bipolar SM circuit is an extension of the HBSM by using flying capacitors. The FCSM has the capability of generating three voltage levels (0, V_C, and $-V_C$). Figure 4c shows the cell structure where four switches

are connected to a clamping capacitor via the upper and lower arms [14]. In the case of an increase in the number of voltage levels, an additional internal voltage balancing for the FCs is required. This SM structure is not attractive for MMCs due to the lack of modularity and reliability [66].

- Double-submodule circuit (DSM) topology: The DSM model was introduced to improve the balancing of capacitor voltages at low switching frequencies. Figure 4d illustrates the basic structure of this SM cell, which consists of two capacitors and eight power switches to achieve three voltage levels. The DSM offers several advantages, including a reduction in capacitor voltage ripple, especially at low switching frequencies, and a reduction in size and cost [67].
- Clamp-double circuit (CDSM): As shown in Figure 4e, the CDSM topology consists of two HBSMs connected in series through two diodes and additional integrated IGBT switch S_5 in the middle. During the normal operation of CDSMs, the middle switch S_5 is always switched on and capable of generating a negative voltage at its output terminal. It includes an increased number of series semiconductors in the conduction path compared to the FBSM. The CDSM configuration also allows the parallel connection of the capacitors within each SM bridge, which results in the low-frequency operation of the MMC topology, as it can reduce the ripple of capacitor voltage [56,67].
- Mix-connected submodule (Mix SM): As shown in Figure 4f, the structure of the Mix SM combines the HB and FBSM topologies to generate the necessary negative polarity voltage for DC-side fault blocking. It can be considered as a hybrid configuration topology operating as HBSMs during the steady state. During faults, the HB leg provides voltage and current blocking as required [53].
- T-submodule 1 (TSM1): The TSM1 and TSM2 topologies are designed for modular multilevel-converter-based HVDC systems. Figure 4g shows the TSM1 circuit, which consists of two unidirectional IGBTs with antiparallel diodes, one four-quadrant bidirectional switch in a common emitter configuration, and two capacitors (C_1 and C_2), whose voltages are controlled to be equal. TSM1 can generate three voltage levels (V_C, $V_{C/2}$, and 0) depending on the full-on, half-on, and bypass states. The new TSM topologies add additional benefits such as reduced voltage stress across the extra inserted switch and considerably lower semiconductor losses compared to the traditional HBSM. However, both the TSM1 and TSM2 topologies have shortcomings against DC faults [43].
- T-submodule 2 (TSM2): TSM2 is unlike the HBSM topology as it only produces two voltage levels. Figure 4h shows TSM2, which operates similarly to TSM1. The SM structure comprises two unidirectional IGBTs with antiparallel diodes, with conduction occurring through two antiparallel diodes and an IGBT switch, and two capacitors (C_1 and C_2), whose voltages are controlled to be equal. Three voltage levels (V_C, $V_{C/2}$, and 0) can be generated depending on the switching states. The power losses in the TSM2 topology are higher than in TSM1, but this eliminates the need for an additional IGBT [43].
- Cross-connected submodule (CCSM): As shown in Figure 4i, this SM consists of two half-bridge cells connected back-to-back in a crossed fashion via the cross-switches (S_5, S_6). Depending on the different switching states, this structure is able to generate a symmetrical five-level output voltage of $2U_{dc}$, U_{dc}, 0, $-U_{dc}$, and $-2U_{dc}$. This SM topology has the capability of blocking a short-circuit current. However, the ratings of the semiconductors for the cross-switches and the comparatively high count add some complications to the CCSM configuration [68].
- Semi-full-bridge submodule (SFBSM) topology: The SFBSM topology is an extension of the CDSM model with some differences. Instead of two diodes, active switches are used, which changes the submodule's function and operating principles. The SFBSM configuration consists of two FB cells with two capacitors in both cells. These capacitors can be connected in parallel with both positive and negative polarity, which can

increase the modulation index above unity or provide more voltage levels with fewer capacitors. However, there may be a slight difference between the capacitor voltages due to differences in the capacitance values, resulting in a current spike when they are connected in parallel. This can lead to some energy losses, but they are generally small [64,69].

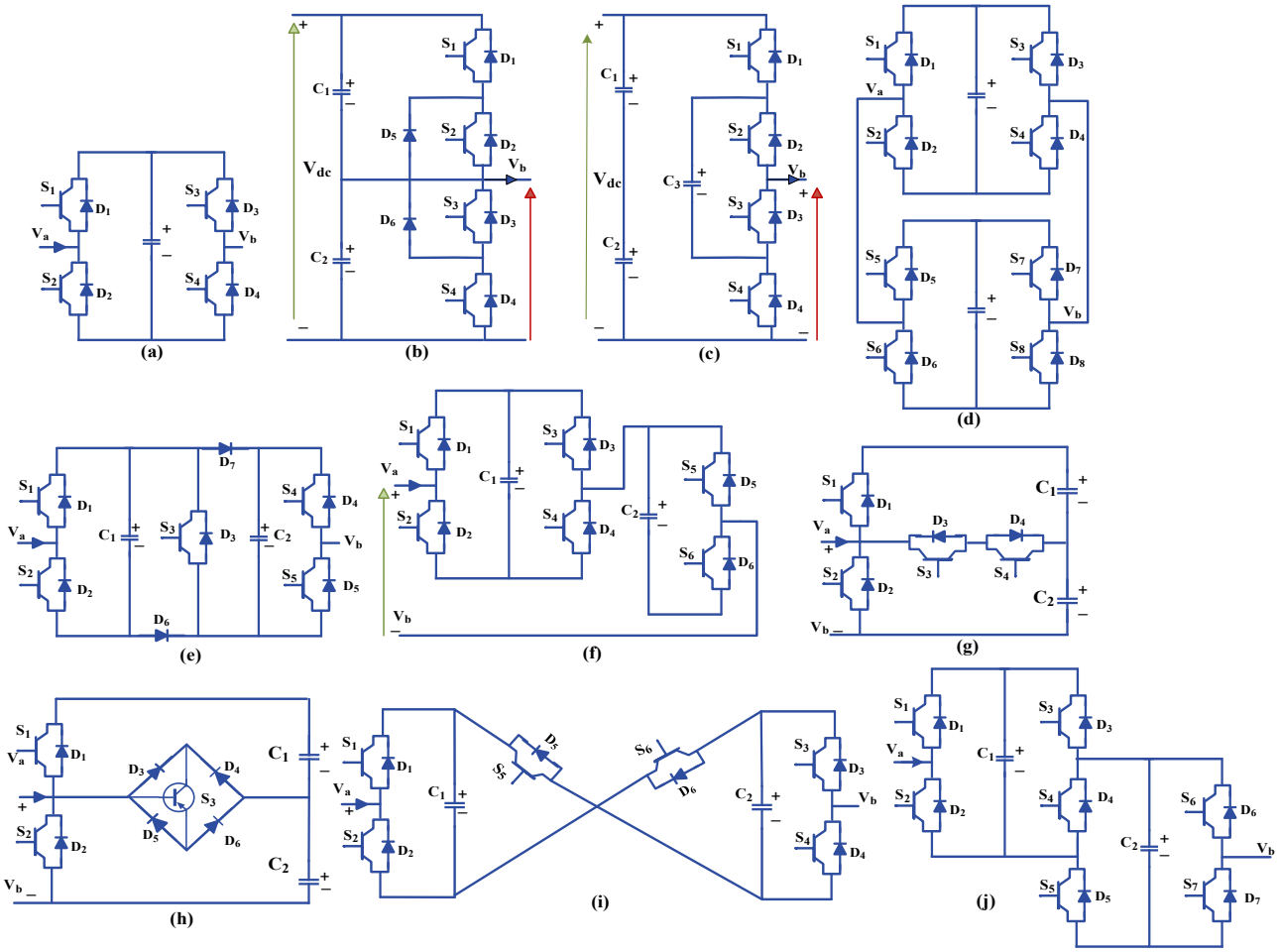

Figure 4. Bipolar SM structures. (**a**) FBSM, (**b**) DCSM, (**c**) FCSM, (**d**) DSM, (**e**) CDSM, (**f**) Mix SM, (**g**) TSM1, (**h**) TSM2, (**i**) *CCSM*, and (**j**) SFBSM [70,71].

2.2.3. Other MLI Topologies

During the past few decades, several inverter and SM topologies have been reported because of different application requirements. Some of the classical and developed MLIs that could not be covered in the previous sections are briefly summarised as follows:

- Cascaded H-bridge multilevel inverter (CHB-MLI): The first CHB-MLI was suggested by Baker and Bannister in [72]. The basic model of the CHB inverter consists of a series connection of H-bridges with separate DC sources, as shown in Figure 5a. By cascading a number of H-bridge cells and each cell being supplied by an isolated DC source, a high number of voltage levels can be generated theoretically. The CHB-MLI topology offers several benefits. Firstly, it has a compatible structure, which makes it easy to modulate, control, protect, and maintain during failures. Secondly, it can handle higher voltages without voltage imbalance. Thirdly, it can eliminate common-mode voltages by selecting the proper modulation scheme. Fourthly, it produces an almost sinusoidal output, which means that an output filter is almost unnecessary. Fifthly, it requires fewer components compared to other topologies.

Sixthly, it does not require flying capacitors or clamping diodes. Lastly, it has a uniform distribution of load power among all switching devices. Despite these advantages, this topology has some serious drawbacks such as requiring numerous separate DC sources and many DC link voltage controllers. The CHB-MLI topology finds applications in various fields, including the RER interface, motor drives, electric vehicle drives, laminators, blowers, fans, conveyors, DC power source utilisation, frequency link systems, and power factor compensators [71,73].

- Packed U cell inverter (PUC) topology: The PUC topology consists of packed U cells, and each U cell comprises an arrangement of two IGBT power switches connected via one capacitor, as shown in Figure 5b. This type of inverter is capable of generating a seven-level voltage at its output terminal. The PUC offers high-energy conversion quality using a small number of power devices and capacitors, resulting in a low production cost [74]. Recently, a new configuration of a single DC source hybrid packed U cell (H-PUC) converter was proposed in [75]. This topology requires one DC source, twelve IGBT power switches, and three capacitors to provide a 23-level output voltage. Figure 5c shows the circuit structure comprising two high-voltage, low-frequency (LF) and low-voltage, high-frequency (HF) SMs, which lead to lower power losses and higher efficiency.
- Packed E cell inverter (PEC) topology: In the PEC inverter, the U cells in the PUC inverter are replaced by E cells, which are packed cell structures. The E cells consist of two capacitors, which are shunted by a four-quadrant switch to form a single cell, as shown in Figure 5d. The two capacitors are actively balanced and simultaneously charged or discharged with redundant states to achieve nine voltage levels. The basic idea behind the E cells is to use a combination of capacitors and switches to achieve multiple voltage levels with fewer semiconductor devices. By using two capacitors in a shunt configuration, the E cell can be charged or discharged to one of nine possible voltage levels, depending on the state of the four-quadrant switch. One of the main advantages of this topology is that it reduces the number of semiconductor devices required compared to the PUC topology, which leads to lower power losses and cost. Additionally, the active balancing of the capacitors helps to ensure that the voltage levels are accurately maintained, resulting in a more-stable output voltage [76]. In addition, the boost packed E cell (BPEC) inverter was recently proposed based on the conventional PEC topology [77]. The single-phase BPEC is capable of generating a symmetrical 11-level voltage waveform using eight IGBT power switches and three DC capacitors in two DC links. The bottom two capacitors are connected in series and form the second DC link. This inverter topology is suitable for flexible AC transmission systems (FACTSs) and active power filter (APF) applications due to its multiple advantages, such as boost performance, low harmonics, low-voltage DC link, low-voltage stress, fault tolerance, and small size filter requirements. These advantages make the BPEC an affordable and reliable inverter.
- Series-connected switched-source multilevel inverter (SCSS-MLI): The SCSS-MLI topology involves connecting voltage sources in series using power switches. A diagram of this configuration is shown in Figure 5e. The semiconductor power switches are connected to the poles of the voltage sources with lower magnitudes, and they are also connected to the poles of the voltage sources with higher magnitudes from an upstream source. This link is capable of synthesising a DC voltage with multiple levels, considering both polarities using the H-bridge. This structure reduces the number of switches required for the symmetrical inverter structure. However, this topology has several drawbacks, such as requiring power semiconductors with the same rating, making load sharing impossible due to various input stage configurations, and high-rated switches that need to be switched at the minimum possible frequency [73].
- Nilkar multilevel inverter (N-MLI) topology: Figure 5f illustrates the basic module of the N-MLI, which consists of four IGBT power switches and two identical DC voltage

sources with four semiconductor switching units for generating a staircase DC voltage waveform with positive polarity. The N-MLI can generate more voltage levels at the output terminal. In comparison with other classical MLI topologies such as the CHB, NPC, and FC multilevel inverters, the N-MLI offers additional advantages such as a smaller number of power switches, leading to the reduction of the size and power loss, a low THD, high efficiency, and a simple gate drive and control strategy [78].

- Reversing-voltage multilevel inverter (RV-MLI) topology: The idea of the reversing-voltage MLI topology was initially proposed by Najafi et al. This topology generates a sinusoidal output voltage in both the level-generation and polarity-generation stages. The level-generation stage produces positive voltages, while the polarity-generation stage produces negative voltages, as illustrated in Figure 5g. This topology can be expanded to include any number of levels, allowing it to be applied to three phases as well. It offers flexibility in terms of switching sequences and requires only a few components to function, making it useful in applications such as FACTSs and HVDC. However, using different DC sources is not feasible in this topology because it is impractical to combine additive and subtractive DC sources [73,79].

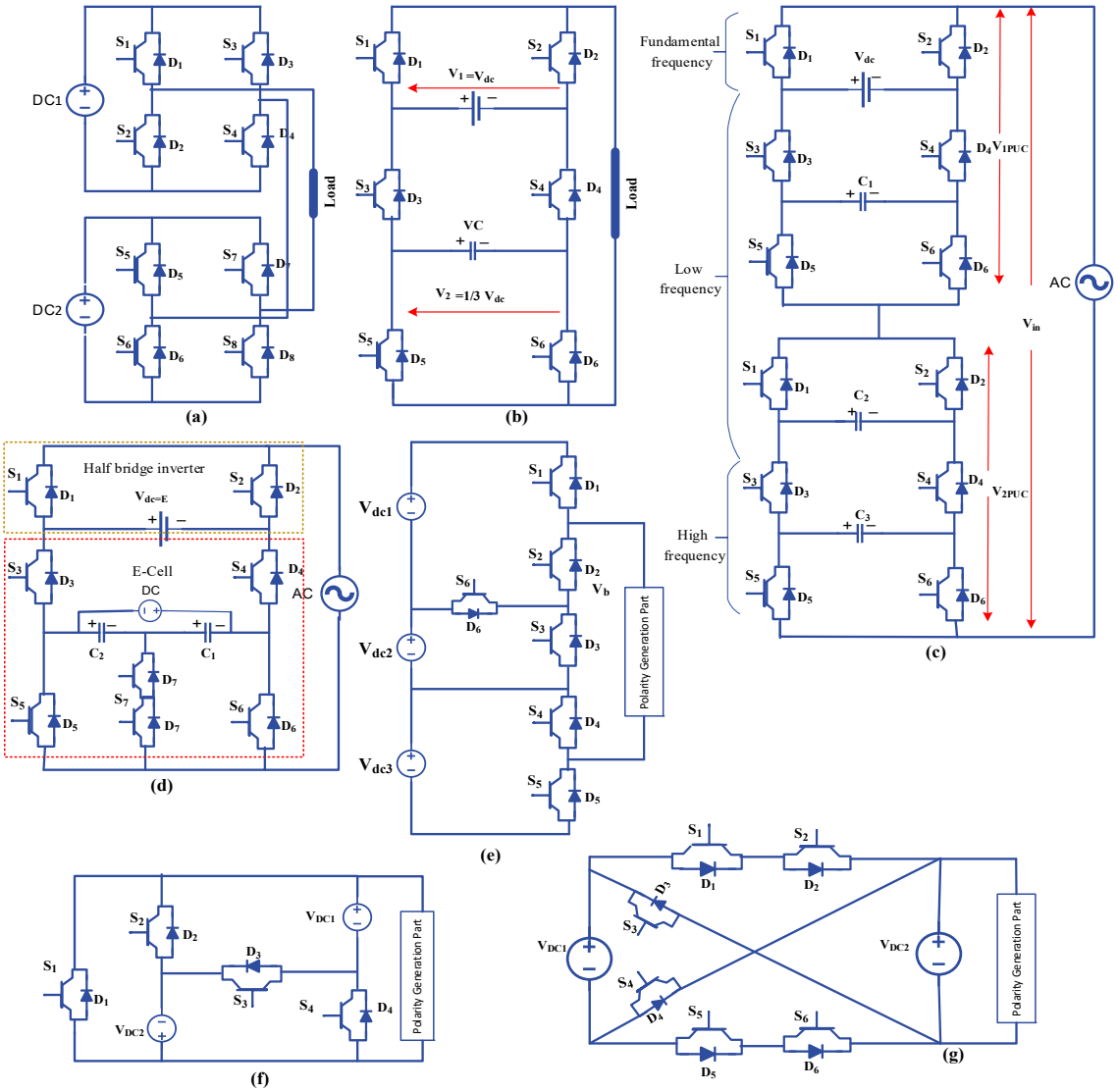

Figure 5. MLI topologies: (**a**) CHB, (**b**) *PUC*, (**c**) *HPUC*, (**d**) PEC, (**e**) *SCSS-MLI*, (**f**) *N-MLI*, and (**g**) *RV-MLI* [73].

Different converter topologies have been published, as mentioned in the previous section, with varying sizes, different control systems, and varying output voltage levels from two-level to multi-voltage levels. Each converter topology has its own advantages and drawbacks. Table 1 presents a comprehensive summary of the advantages and disadvantages of several common MLI topologies.

Table 1. A comprehensive summary of the advantages and disadvantages of several common MLI topologies.

Modulation/Control Scheme	Merits	Demerits
MMC [39,40,48,80]	• High quality of voltages and currents • Voltage scalability by cascading more cells • High availability, reliability, and efficiency • Losses are negligible • Switching frequency is low • No AC filters needed • Simple in structure • Capable of independent PQ control	• Uses large number of capacitors and cells • High switching and conduction losses • Balancing of voltage capacitors is required • Complex control • Control unit for circulating current needed
NPC [17,81]	• Back-to-back inverters are employed • Modular in design • Better dynamic response • Absence of floating capacitors • Fewer DC sources needed • Good fault-tolerant characteristics • Acceptable efficiency • Cost-effective	• DC level may discharge due to incorrect control and monitor system • An increase in voltage level needs more clamping diodes • High power losses across inner and outer switches • Costlier and less-reliable • Big volume due to an increase in number of diodes • Harmonics issue
FC [39,82,83]	• Can be employed for fault-tolerant operation • Fewer DC sources needed • Fewer switches devices • Cost-effective if used for high-level structures • Does not require clamping diodes	• Capacitor requirements are more expensive than diodes • Voltage balancing unit is complex • Complication in overall system control • Switching efficiency is minimum • Less reliability • Use of more voltage sensors • Ripples problem at low switching frequencies
CHB [17,71,84,85]	• Structure is simple and modular • Ease of extending to higher levels • Simplicity in storing and packaging • High reliability • Can operate as single DC source unit • Control system is simple • Absence of floating capacitors • Minimum harmonics in the input current • Capability of fault tolerance • Needs only unidirectional switches	• Requirement of more power switches • The level of output voltage is comparatively less • Cost of implementation is large • Voltage rating across switches varies for asymmetric configuration • More DC sources are required • Large number of devices raises the size • High power losses
SCSS [56,73]	• Modular structure • Fewer switches are required • Simple control system	• System only operates in symmetric configuration • Voltage rating varies between devices

	• Rated switches can operate at peak voltage and switching frequency	• Load sharing is not uniform • Large number of DC sources needed • Harmonics issue
N-MLI [73,78]	• Can operate with a smaller number of switches • Less power loss • Less THD • Batteries and capacitors can be used as the DC voltage source	• Complicated structure • Complicated control system • Costly and suffers from high power loss • Not feasible for fault-tolerant operation • High operating temperature exceeds safe levels
RV-MLI [79]	• Three-phase operation can be carried out by single DC link • Non-isolated type of DC links is operated • Fewer power devices • Rated switches are operated at peak voltage and at switching frequency	• Complicated structure • Load sharing is not uniform • Asymmetric configuration is not possible • Complicated control system
PUC [74,75]	• Simple structure • Requires fewer power devices • Simple control system • Possibility of adding more crossover switches	• Atypical structure • Operation with asymmetric configuration • Different switches have different voltage ratings • Fault-tolerant applications are impossible • THD problems • High cost
PEC [76,77]	• Small number of power devices at high voltage levels • Switching frequency can be low • No external complex controller • The challenge of voltage capacitor balancing not required	• Complicated structure • Complex control system • Active capacitor voltage balancing is required • Less reliability
CCHB [56,73]	• Simple structure • Fewer power devices required • The system peak reverse voltage is low • Both symmetric and asymmetric topology are possible • Ability to operate with both positive and negative voltage	• Switches with bidirectional operation are required • Needs isolated input DC link for operation • Complex control system
CCSSM [68]	• Ability to produce possible values of minimum step voltage • Simple structure • Needs fewer power devices • DC-fault-blocking capability	• Requires on-state switches • Operates only with isolated DC sources • Operation at multiple voltage levels with fewer power switches • Not very cost-effective

3. MMC Modulation and Control Techniques

The principle of the MMC topology is based on the differential operation between the DC-side with a voltage of V_{dc} and the total output voltage of DC components at each SM. The differential voltage can be generated by a proper control system for the power devices in each SM. In addition, each phase leg produces a circulating current i_{cc}, which is responsible for transferring the power between the two terminals of the converter. Several control techniques have been used to control the voltage and current of the MMC topology, which have been reviewed in the literature [70]. Figure 6 shows the schematic

diagram of a conventional onshore MMC substation control system for HVDC applications. The conventional control scheme of the grid-connected MMC includes an outer loop control technique for DC voltage control and another inner control for the current tracking. These control strategies specify the reference voltage, which will be generated for each phase leg by using the pulse width modulation (PWM) technique to balance the converter system [86].

Different multilevel converter (MLC) modulation techniques have been used for controlling the flow of the converter voltage and current from both terminals. Figure 7 summarises some of MLC control strategies based on their switching frequency [87]. Each control technology has a different action system to provide a stable converter operating system. However, some control strategies bring real challenges and mostly appear when the number of SMs per arm is increased to raise the voltage levels. Thus, it is important to utilise a suitable control strategy for the MMC model among several control strategies that have been used to achieve the best output power and current via the power converter stage. The modulation techniques come after the control schemes to generate the associated gate pulse signals of the semiconductor devices in the SMs. Thus, these modulation techniques will affect the operation of the total system and will determine the performance of the converter to some extent [41,88]. The most-common modulation techniques will be summarised briefly in the next subsections.

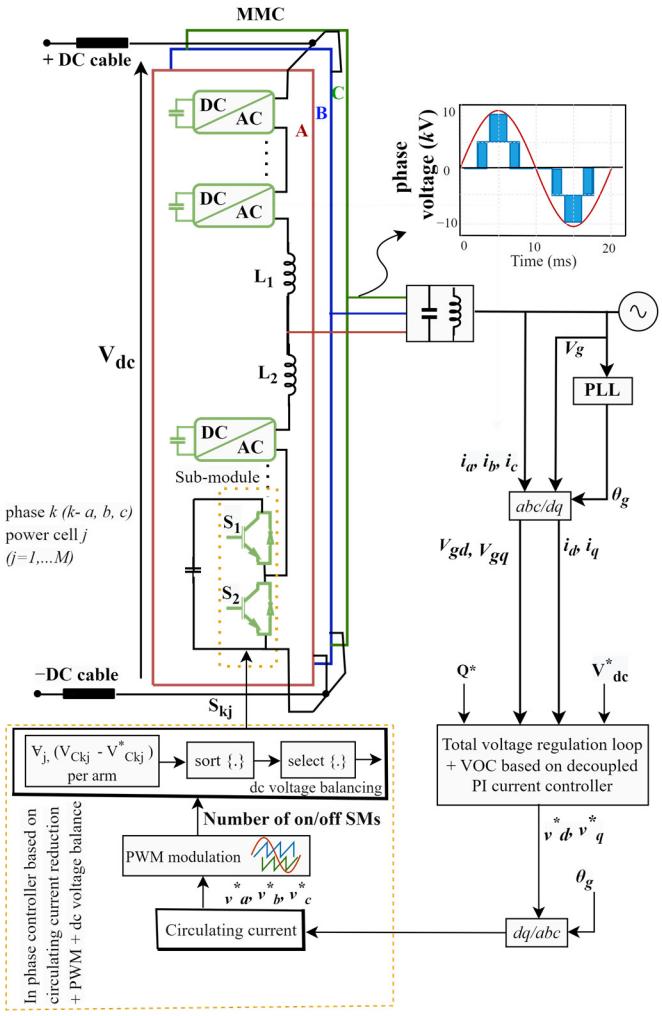

Figure 6. Modulation strategies of a grid-tied MMC topology for HVDC applications. Copied with permission from [86].

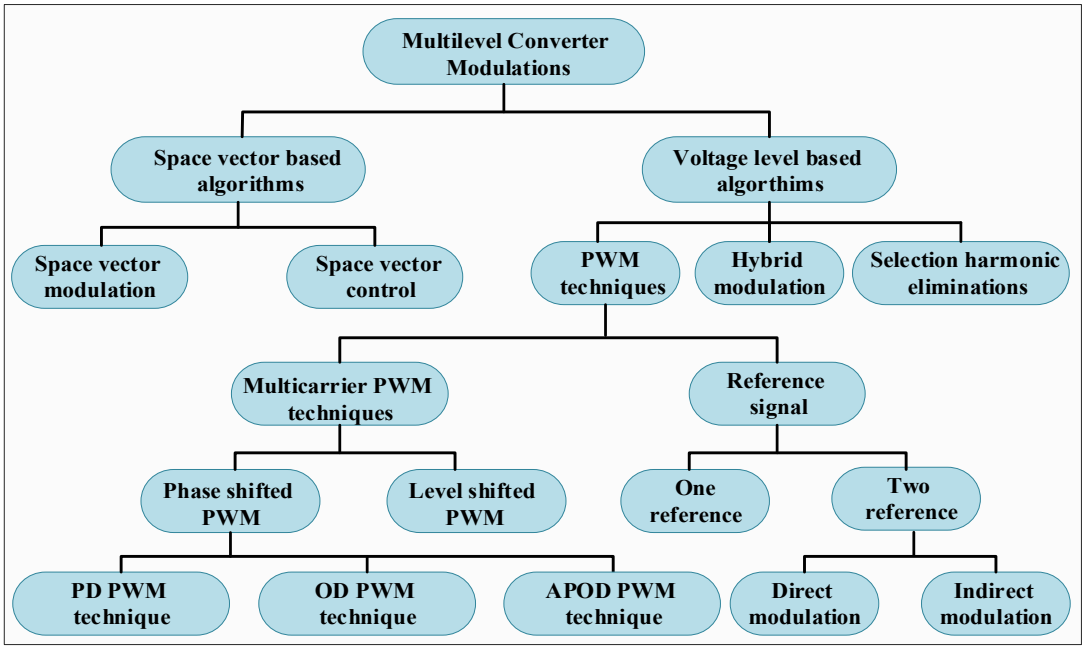

Figure 7. Modulation techniques for modular converter topologies. Copied with permission from [83].

3.1. Multicarrier PWM Techniques

There are some basic requirements for the MMC control system including the control and balance of the SM voltage capacitor and the control of circulating current, which flows through each phase leg to eliminate the harmonics [51]. For example, in the case of using the HBSMs for the MMC topology, the output voltage of each SM VSM is equal to the SM capacitor voltage. VC means that, when the upper IGBT switch is turned on and the bottom IGBT switch is turned off, the SM capacitor will charge or discharge depending on the arm current direction. In the second case, when the upper IGBT switch is turned off and the bottom IGBT is switch turned on, the SM capacitor will be bypassed, and thus, the VSM is equal to zero volts, where each arm in the converter acts as a controllable voltage source and the overall output voltages of the converter are effectively controlled by varying their respective top and bottom arm voltages [48]. Various control strategies have been used for MMC control systems, among which multicarrier PWM techniques such as level-shifted and phase-shifted are developed to reduce the THD of the operation of the MMC topology by comparing a sinusoidal reference signal with a triangular carrier signal, and the gate signals of the power devices are determined directly by a simple comparison of the reference voltage with the carriers [82]. The most-common multicarrier PWM techniques are as follows:

- Level-shifted pulse width modulation (LS-PWM): The gate signals of power devices in each cell are immediately specified by comparing the reference voltage signal with the carrier's signals. N is the number of carrier waveforms required in the control system, where these carriers are placed vertically, and their bands are arranged based on the LS techniques. The total switching of all the SMs in the upper and lower arms of the MMC topology will be equal to the carrier frequency, meaning that the number of SMs can be assumed to be four cells in both arms, in which case four N carriers will be used and vertically distributed from $-V_{dc/2}$ to $V_{dc/2}$ volts, and their magnitude is 0.25 to modify the waveform where the modulating waveform is shifted by fully turning on some of SMs and other SMs being turned off (bypassed) to generate an $N - 1$ voltage level at output side [89,90]. As shown in Figure 6, the most-common multiple carrier level-shifted techniques used for MMC control systems are classified into

the: in-phase disposition (PD PWM), opposition disposition (OD PWM), and alternative opposition disposition (AOD PWM) techniques [91]. Figure 8 shows five level output waveforms of the aforementioned techniques, where in the PD PWM technique, the carrier signals are level-shifted, but all are in same phase. In the POD PWM technique, the positive carrier signals will have a 180° phase shift with the negative carrier signals, and in APOD PWM, the alternate carrier signals will have a 180° phase shift. The PD PWM control strategy has gained wide acceptance in the design of the MMC topology compared to other control technologies as this technique provides load voltage and current with lower losses and less total harmonic distortion (THD) [70].

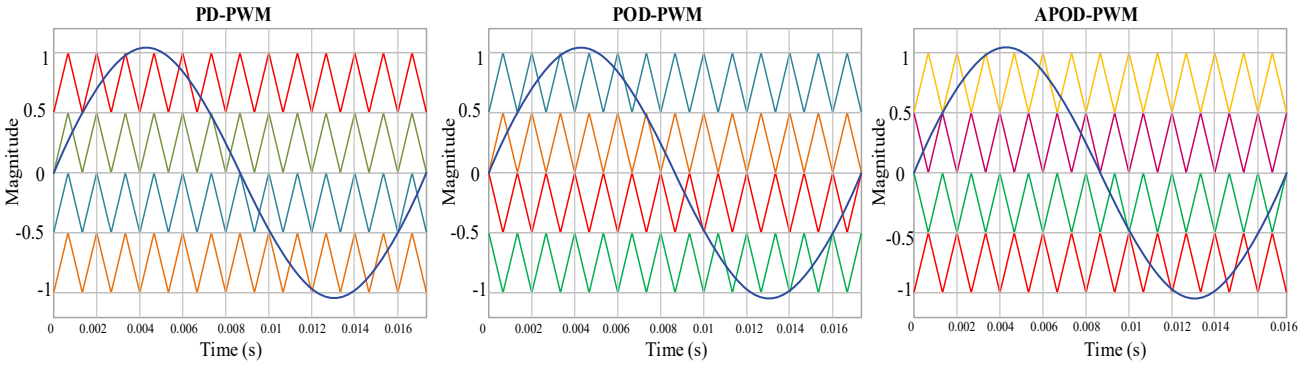

Figure 8. LS-PWM strategies (PD PWM, POD PWM, and APOD PWM). Copied with permission from [87].

- Phase-shifted pulse width modulation (PS PWM): The configuration of the MMC topology is based on connecting a number of SMs, which are used in each phase leg to control the flow of the current and voltage to the load through an integrated system [92]. In this modulation technique, each SM in the MMC topology is controlled separately, and the balancing voltage function for each cell is divided into an averaging control and a balancing control, where $(N+1)$ levels require several triangular carrier waveforms, and all carriers must have the same frequency and peak of the amplitude as there is a phase shift between the adjacent carriers, this shift being given by $\varphi c = 360^{\circ}/N$. Therefore, the waveforms of triangular carriers for each phase are implemented according to the subharmonic techniques [93]. The average voltage at each individual SM capacitor is controlled by the averaging and balancing technique, respectively. The main drawback of the PS PWM technique is that the implementation voltage rises significantly when the number of SMs in each arm phase is increased, which leads to instability under certain operating conditions [94].

3.2. Direct Modulation

In this modulation technique, the upper and lower arm voltages of phase j will be controlled by two complementary sinusoidal reference waveforms as given by:

$$n_{P,j,ref} = N\frac{\frac{V_{ds}}{2}+v_{j,ref}}{V_{dc}} \quad (1)$$

$$n_{N,j,ref} = N\frac{\frac{V_{ds}}{2}+v_{j,ref}}{V_{dc}} \quad (2)$$

where $v_{j,ref}$ represents the reference output voltage of phase j and $n_{P,j,ref}$ and $n_{N,j,ref}$ are the reference waveforms for the number of inserted SMs in the upper and lower arms, respectively. The reference waveforms in Equation (1) are compared with the PD PWM carrier waveforms, which vary between 0 and N, to determine the required number of inserted SMs for each arm. The major drawback of the direct modulation technique is the

presence of circulating current, which is responsible for system instability and increases the converter power losses [41].

3.3. Indirect Modulation

In this technique, the upper and lower arm reference waveforms of phase *j* are given by the following equations.

$$n_{P,j,ref} = N \frac{\frac{V_{ds}}{2} + v_{j,ref} - v \sum_{reg,j} - v_{reg,j}^{diff}}{\sum_i^N v_{cp,i,j}} \quad (3)$$

$$n_{n,j,ref} = N \frac{\frac{V_{ds}}{2} + v_{j,ref} - v \sum_{reg,j} - v_{reg,j}^{diff}}{\sum_i^N v_{cn,i,j}} \quad (4)$$

where $v \sum_{reg,j}$ and $v_{reg,j}^{diff}$ are used to control the total energy in the phase *j* leg and can balance the energy between the upper and lower arms, respectively; $v_{cp,i,j}$ and $v_{cn,i,j}$ represent the capacitor voltage of the upper and lower SMs of phase *j*. Similar to the direct control, the reference signal waveforms can be compared with the waveforms of the PD PWM carrier to determine the number of inserted SMs in both arms [87,95].

3.4. Closed Loop Control Technique

Closed loop control can be used to reduce the capacitor voltage ripples and the power losses of the MMC topology. Based on Equations (3) and (4), the term $\sum_i^N v_{cx,i,j}$ is calculated based on the actual measured capacitor voltages $v \sum_{reg,j}$ and $v_{reg,j}^{diff}$, which results in the total energy stored in the phase *j* leg and also the balance of the voltage capacitors between the two arms subtracted from the output voltage reference e_v^{ref} as follows [87].

$$v_{CU}^{ref} = \frac{V_{ds}}{2} - e_v^{ref} - v \sum_{reg,j} - v_{reg,j}^{diff} \quad (5)$$

$$v_{CL}^{ref} = \frac{V_{ds}}{2} + e_v^{ref} - v \sum_{reg,j} - v_{reg,j}^{diff} \quad (6)$$

The controller will balance the cell voltages using the circulating current i_{diff} through each phase leg, as shown in Figure 9 [41]. The control of the circulating current within both arms can be achieved by the voltage difference applied from the DC source and across the SM capacitors [96]. One of the most-important benefits of the closed loop control technique is that it allows for the accurate monitoring and regulation of the converter output voltage with the flexibility of increasing the number of voltage levels, and it also has the capability of controlling the imbalance of the energy between the upper and bottom arms easily [97].

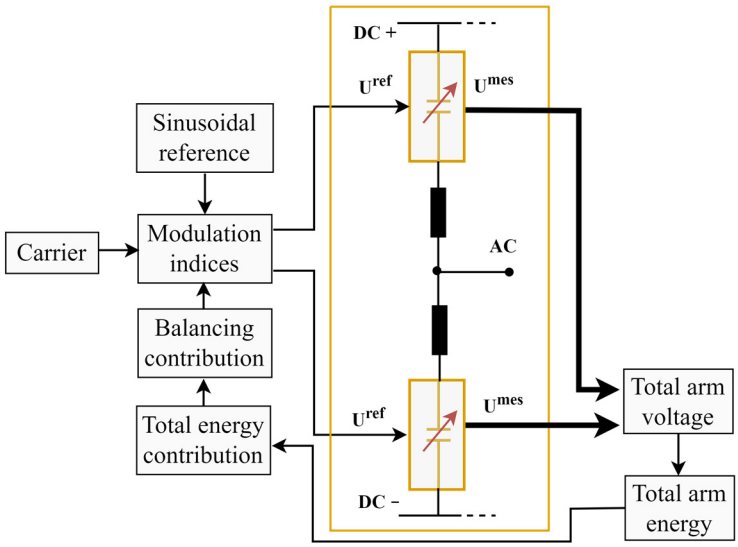

Figure 9. Schematic diagram of closed loop control technique. Copied with permission from [41].

3.5. Open Loop Control Technique

This controller, also known as the non-feedback system, provides the required output by evaluating its input and has become one of the popular control techniques that have been used for several power converters due to its simple structure, quick operation, low maintenance requirements, and cost effectiveness. The operation of the open loop control system is based on the estimation of the total capacitor voltages via the stored energy in each arm's SMs, which is performed by measuring the other components and results in a less-complex interface with the regulator. The contribution of the voltage difference v_{diff} that must be deducted from the voltage reference e_v^{ref} can be described as follows [86,98].

$$v_{CU}^{ref} = \frac{V_{ds}}{2} - e_v^{ref} - v_{diff} \quad (7)$$

$$v_{CL}^{ref} = \frac{V_{ds}}{2} + e_v^{ref} - v_{diff} \quad (8)$$

Figure 10 shows the configuration of the open loop control system. The operation of this control technique is flexible and can be achieved by measuring the output voltage and current, as this process depends on the solution of the steady state technology, where the above equations described the dynamics and mechanism of the converter behaviour and ensure a stable operating system with fewer harmonics in each phase leg current. The closed loop approach is more suitable for use in MMC topologies because of its reliability, and it has significantly lower sensitivity to changes in the system parameters and generates an oscillation-free response compared to an open loop control system [41,99].

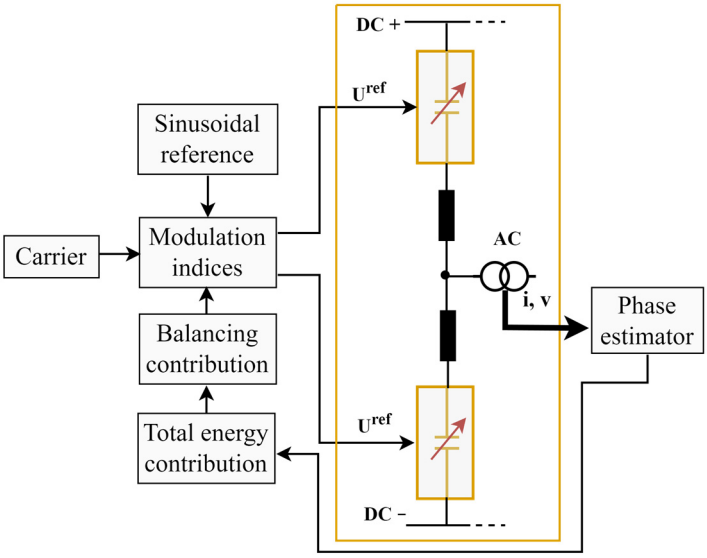

Figure 10. Schematic diagram of open loop control technique. Copied with permission from [41].

3.6. Selective Harmonic Elimination Technique

The SHE technique was first introduced in 1973 [100]. It is a practical approach for reducing the harmonics in power converters, including the MMC topology. By employing the SHE method, it is possible to eliminate the THD and reduce the size of the output filter. The fundamental concept of SHE techniques is based on the Fourier series analysis of the PWM voltage/current waveform, which depends solely on the characteristics of the given waveform, where SHE-PWM involves decomposing the periodic PWM voltage waveform generated by a power electronic converter using Equation (1) and determining the switching angles (αi) that can control or remove the selected low-order harmonics. The literature has explored various waveform formulations, as depicted in Figure 11. The simplest SHE-PWM problem formulation for both two-level and multilevel waveforms assumes quarter-wave symmetry (QW) waveforms [101,102].

$$f_N(t) = \frac{a0}{2} + \sum_{n=1}^{N} \left(a_n \cos\left(\frac{2\pi nt}{T}\right) + b_n \sin\left(\frac{2\pi nt}{T}\right) \right) \quad (9)$$

The SHE method offers important functions such as preserving the basic waveform, reducing the harmonics, minimising the THD, and decreasing the switching losses. Nonetheless, a significant drawback of this technique is the need for large passive filters to restrict the lower-order harmonics, as mentioned in [103]. To overcome this limitation, researchers have introduced a new method called selective harmonic mitigation (SHM), as described in [104].

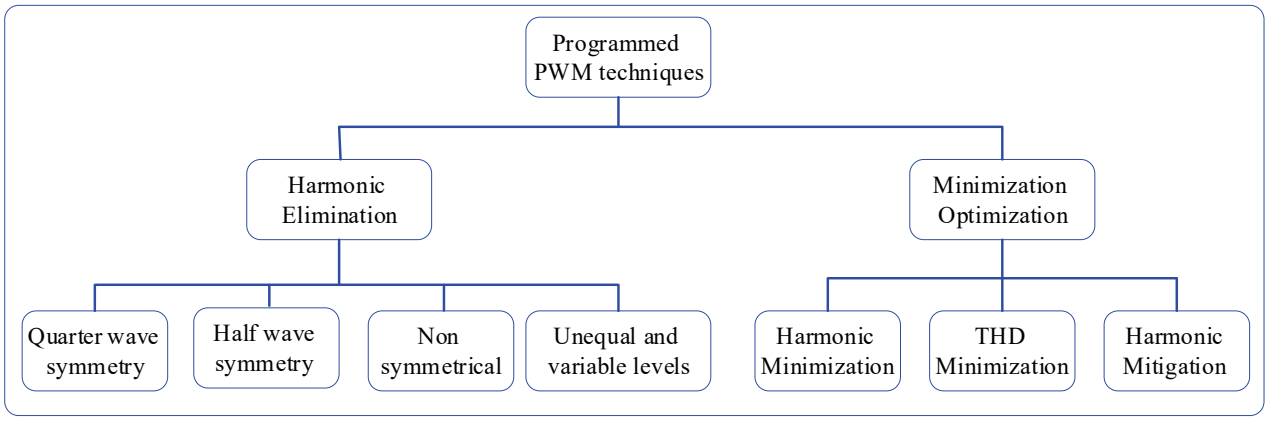

Figure 11. Classification of SHE-PWM formulations. Copied with permission from [102].

3.7. Space Vector/Nearest Vector Control

Space vector control (SVC), also known as nearest vector control (NVC), is a technique that can be used instead of SHE. NVC can operate at lower switching frequencies and, like SHE, does not generate the average value of the required load voltage for each switching time interval. NVC's primary function is to choose a vector closest to the reference vector to minimise the distance between them or the space error [105]. However, the lower distortions produced due to the low-frequency switching in NVC are usually not eliminated, unlike in SHE. The NVC technique is simple and useful for higher output voltage levels since the higher density of the vectors can generate only small errors about the reference vector. In [106], the authors discussed the principle of an eleven-level inverter with SVC. Recently, SVC has been implemented in various multilevel inverters (MLIs), including both classical and the newly proposed reduced switch count technology. In [107], a five-level MLI configuration with a quasi-Z-source was designed, and NVC was employed as the control scheme.

There is an algorithm that has been developed with the ATmega64 microcontroller architecture in mind. This microcontroller provides phase-corrected PWM, which generates a symmetric PWM. A timer overflow interrupt is generated when the timer counter register's (TCNT) value matches the input capture register's (ICR) value. In the interrupt service routine, all necessary calculations for generating the duty cycle for each leg are performed. Figure 12 illustrates the algorithm used to calculate the duty cycle [108].

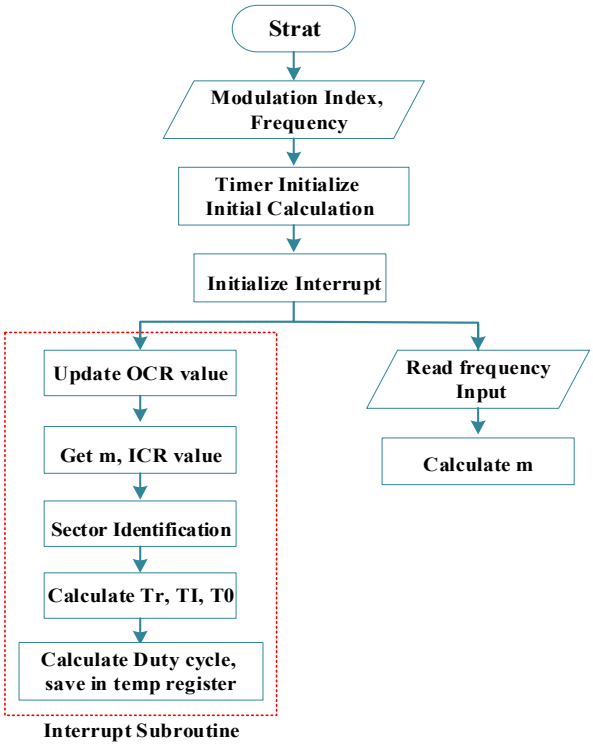

Figure 12. An algorithm of duty cycle calculation. Copied with permission from [108].

3.8. Model Predictive Control

Model predictive control (MPC) has recently gained popularity as a powerful tool for controlling high-power multilevel converters [109]. MPC eliminates the need for PI regulators and pulse width modulators, resulting in improved dynamic response and controllability. Additionally, MPC is easy to design, robust to changes in the system parameters, and can handle system constraints and nonlinearities. MPC can also compensate for control delays and achieve multiple control objectives using a cost function. As a result, MPC is widely used to control various MLI topologies, including NPC, FC, CHB, and matrix converters. Recent studies have shown that MPC is highly effective at controlling the output currents, SM capacitors' voltage, and the circulating current of an MMC by using a cost function. Figure 13 illustrates the diagram of the MPC technique [110,111].

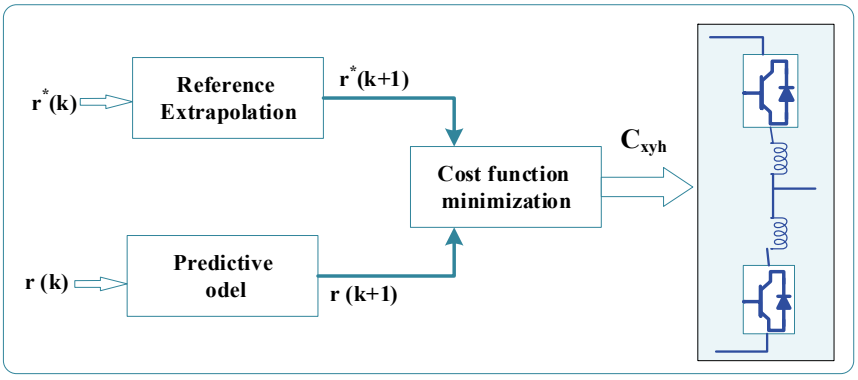

Figure 13. Diagram of MPC technique. Copied with permission from [111].

Modulation and control techniques are integral to the operation of power electronic systems, particularly inverter systems. These techniques are used to regulate the output voltage and current of the inverter and ensure efficient operation of the system. One of the primary functions of MLI modulation and control techniques is to reduce the level of the

harmonics in the output waveform. Harmonics are unwanted frequencies that can cause problems in power electronic systems, such as overheating and increased losses. By using appropriate modulation and control techniques, the level of harmonics can be reduced, improving the overall efficiency and reliability of the system. The control techniques are also responsible for generating reference control signals that maintain the balance of the voltage sources. In MLI systems, for example, multiple voltage sources are used to generate the output waveform. Modulation techniques ensure that these voltage sources are balanced and that the output waveform is of the desired shape and amplitude. Therefore, the choice of control system can have a significant impact on the performance of the inverter system. The main merits and demerits of MLI modulation and control techniques are summarised in Table 2.

Table 2. Brief comparison of MLI modulation and control techniques.

Modulation/Control Scheme	Merits	Demerits
Open loop system [41,98]	• Simple and economic structure • Requires lower number of components • Fast response ability • Good stability	• Unreliable system • Accuracy depends on calibration • System disturbance issues • System improvement is not possible
Closed loop system [96,97]	• Reliable system • The feedback element is always present • An error detector is always present • More-accurate system	• Complicated structure • It may become unstable • Lower response ability • High cost
Phase-shifted PWM technique [86,88,89]	• Modular and simple structure • Better voltage output • Optimal switching is achieved • Rotation of switching patterns is not required • All carriers have the same frequency and amplitude	• Poor dynamic response • Poor voltage balancing strategy • Harmonic issues
SHE technique [100–102]	• Appropriate for high power application • Better steady state response • Reduced output filter size • Ability to eliminate lower-order harmonics • High efficiency • Low losses during switching operation • Low harmonics	• Requires massive passive filters • Low overall dynamic response • Ineffective voltage balancing operation
SVC technique [106,108]	• Simple technique • Fewer switching states • Can operate at low switching frequency • Lower dv/dt stress • Low harmonics with high efficiency • Does not require huge passive filters • Better dynamic response	• Complex for structures involving more voltage levels • Lower-order-harmonics-clearance problem
MPC technique [109,111]	• High-efficiency performance • Cost-effective and enhanced energy saving • Enhanced transient response • Prediction of upcoming disturbance • Upcoming control actions' prediction • Peak load shifting capability	• High-cost installation system • Computational complexity • Needs improvement of mathematical and analytical model • Needs identifying a proper model of the system

4. WBG Semiconductor Device Technology

In this section, the most-promising commercial WBG power devices are reviewed to discuss their deployment in the MMCs. Since the invention of the transistor, semiconductor devices based on the Si material such as MOSFETs and IGBTs have been widely used in several power applications due to their acceptable performance, wide availability, and affordability [112–114]. However, it seems that the performance of Si-based power devices has reached its maturity, and several limitations appear when considering the growing energy needs. Some of these limitations are high power losses, a low switching frequency, and a poor high-temperature performance, generally having a power density limit of 200 W/cm^2 and a peak temperature of less than 150 °C [115]. Semiconductor materials that have a larger energy bandgap than the Si material are known as superior materials for fabricating high-temperature and high-speed electronic devices. WBG semiconductor materials, which have a bandgap much greater than those of traditional semiconductor materials, have been used in the first and second generations to allow semiconductor power devices to operate at higher frequencies and higher voltages, and also permit the temperature to reach around 300 °C [116,117]. There are several WBG materials currently being explored for power conversion including SiC- and GaN-based devices, which are recognised as an effective solution for future power electronic systems [118,119]. Table 3 summarises the main parameters and specifications of the WBG semiconductor materials compared to the Si materials. The WBG devices are expected to dominate the power electronics markets in the near future [120].

Table 3. The materials of WBG power semiconductors compared to the Si material. Copied with permission from [120].

Properties	1st-Generation	2nd-Generation	3rd-Generation	
	Si	GaAs	SiC	GaN
Energy bandgap E_G (eV)	1.12	1.4	3.2	3.5
Breakdown field E_B (V/cm) × 10^6	0.3	0.4	2.2	3.3
Saturation drift velocity v_s (cm/s) × 10^7	1	2	2.7	2.7
Thermal conductivity (W/cmK)	1.5	0.5	4.9	2.3
Permittivity ε_r	11.8	12.8	9.7	9.5
Electron mobility μ_n (cm^2/V$_s$)	1500	8500	650	900–2000

Based on the parameters listed in Table 2, the incorporation of the WBG technology into power semiconductors has proven itself to be superior to that of traditional Si-semiconductor-based device technologies [119]. The SiC and GaN WBG materials are being utilised in power semiconductor manufacturing and are expected to be an attractive solution for several electronic power applications such as photovoltaics (PV), DC–DC converters, DC–AC inverters, motor drives, battery chargers and adapters, electric vehicle (EV) propulsion converters and chargers, switched-mode power supply (SMPS), and several other industrial applications because WBG-based devices provide powerful characteristics, as shown in Figure 14 [121]. For instance, they offer a higher electric breakdown field, which enables a greater voltage blocking capability, thinner layers, a deeper doping concentration, and a lower on-resistance ($R_{DS\,(on)}$) value compared to Si-based devices. This results in lower switching and conduction losses. With the same $R_{DS\,(on)}$, the WBG devices can have a smaller area, which means less capacitance with a higher saturation drift velocity, which allows higher switching speeds and lower losses per switching cycle [32]. Moreover, WBG devices allow simplifying the converter circuit topologies by reducing the size and number of passive components such as capacitors and inductors, which play an important role in reducing the leakage currents and have a strong influence on the performance at high temperatures [122,123].

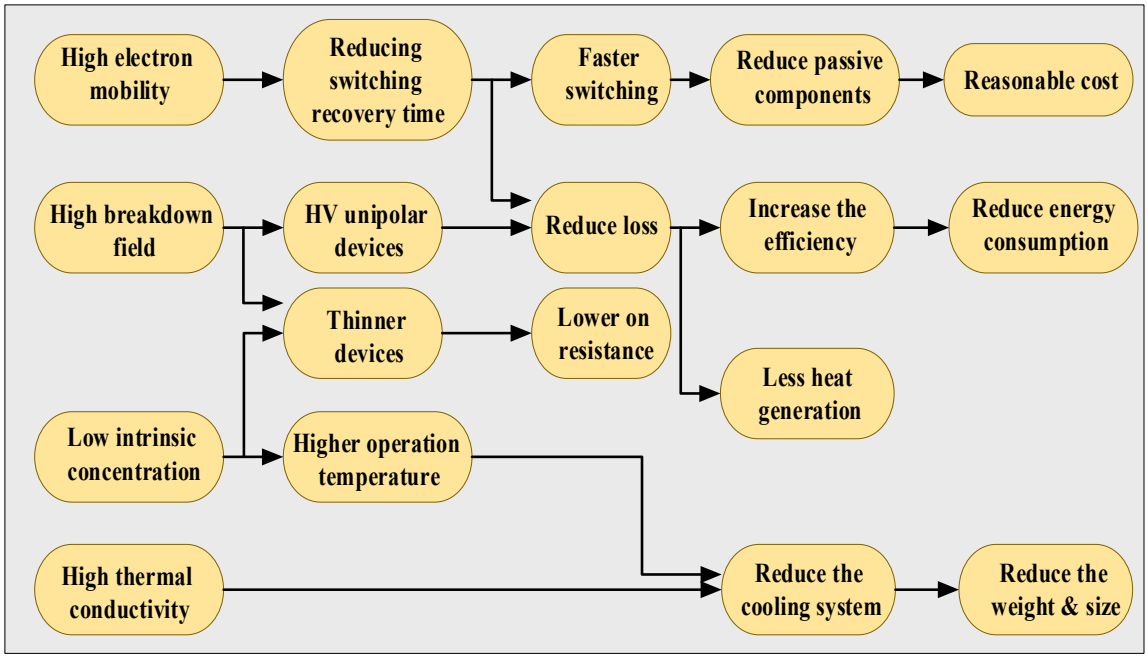

Figure 14. Diagram of WBG materials' properties. Copied with permission from [32].

4.1. SiC Technology

SiC devices are a part of the WBG semiconductor materials' family with the capability of meeting the growing performance requirements in the design of several advanced power applications such as high-power devices with high-frequency-based power converter topologies [124,125]. During the last two decades, the development of switch devices based on the WBG-SiC materials has gained more attention, and they are expected to be among the alternative materials to the conventional Si devices for future power applications. The SiC technology has provided many advantages such as increasing the switching frequency, increasing the breakdown voltage, operating at higher temperatures, and reducing the power losses [126]. Figure 15 shows different typical types of SiC devices such as the Schottky barrier diode (SBD), metal–oxide silicon field-effect transistors (MOSFETs), the depletion-mode MOSFET (DMOSFET), and insulated gate bipolar transistors (IGBTs) [20]. These devices allow the optimisation of many aspects in the energy conversion system as follows [122,127]:

- At the converter level: by directly replacing the Si devices by SiC ones or simplifying the circuit topologies to improve the converter efficiency, fast switching capabilities, low power loss, and reducing the active and passive component numbers to reduce the converter size.
- At the system level: converter topologies based on SiC switches are able to provide a better dynamic performance, high frequency capability, and high bandwidth enabled by the fast switching speed.
- SiC can enable new applications such as solid-state transformers (SST) with high-efficiency and high-density, as well as high-speed motor drives. Recently, several commercial and research prototype inverters using SiC devices have been developed with promising results, which have shown a significant improvement in efficiency and power density.

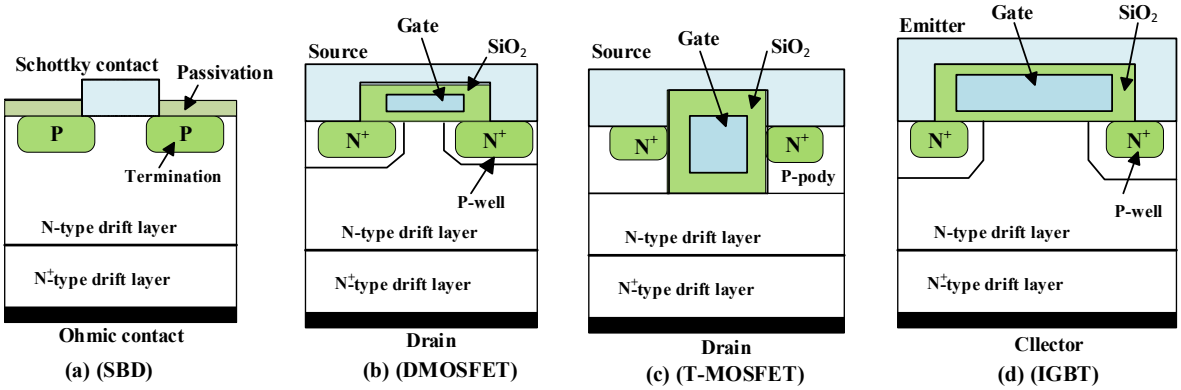

Figure 15. Types of SiC devices: (**a**) SBD, (**b**) DMOSFET, (**c**) MOSFET, and (**d**) IGBT [128].

4.2. Development of SiC Power Devices

Recently, adopting high-voltage SiC devices can improve the performance in terms of a fast switching speed, low specific on-resistance, high voltage rating, and higher temperatures, theoretically up to 300 °C [128]. In general, the first real deployment of the SiC-based devices as an electronic substrate material date back to the late 1950s. However, the research work in the power electronics field began to gain momentum in the late 1980s and early 1990s when Nishino and Powell developed the heteroepitaxial growth of SiC crystals on Si substrates [129]. Furthermore, several high-voltage diodes and junction-controlled devices have been invented during the past few decades, among which the MOSFET was proposed 1989 [130,131]. Thereafter, the first 750 V 6H-SiC-MOSFET and 1100 V 4H-SiC-MOSFET were published in 1997 [132,133]. Now, SiC-based devices are becoming more attractive due to the increasing demand for power integration systems, and researchers are employing SiC-based MOSFETs in several power applications such as motor control, electric power transmission, electric hybrid vehicles, and power management [134]. Figure 16 shows the development of SiC power devices in the last 22 years; as early as 2001, Infineon produced the first commercial SiC-SBD with the characteristics of high blocking voltage, better thermal stability, and hardly any reverse recovery time. Due to the continuous progress, the SiC devices are employed at a greater pace in various countries presently [126,135]. Currently, it is possible to find SiC-based devices such as JFETs, BJTs, and MOSFETs available at various rated voltage levels from 600 V to 1.7 kV and current ratings from 2 A to 325 A, which makes them suitable for high-voltage applications [27].

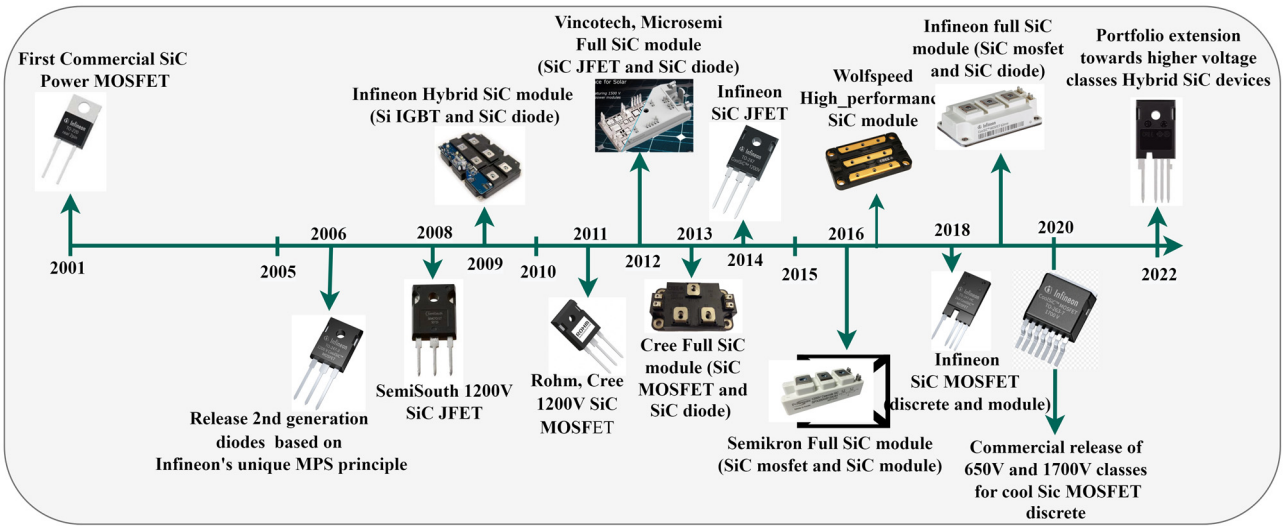

Figure 16. The development of SiC devices' technology. Copied with permission from [126].

4.3. SiC's Key Challenges

Despite the superior properties of the SiC devices, which have led to the rapid growth of their employment, there are still some challenges and problems that need to be considered and solved. Many manufacturing efforts are moving towards further optimisation of the SiC devices in terms of reducing their cost. Although some challenges facing the development of the SiC devices have been largely overcome, the following challenges still need consideration [24,126]:

- SiC wafer and substrate fabrication: A SiC wafer is a semiconductor material that has excellent electrical and thermal properties. However, the SiC wafer has some drawbacks such as crystallographic defects within the wafer, and surface defects at or near the wafer surface still remains a challenge for manufacturers as improving SiC wafer quality is important for manufacturers because it directly determines the performance of the SiC devices [136].
- SiC physics and device development: This means the development of the theoretical design of SiC-based devices, as well as the practical problems associated with the planning, fabrication, and construction of device circuits or integrated circuits (ICs). The related issues that need some improvements are: (i) the ohmic contacts and (ii) the strong dielectric oxide layers, whereas the essential step for making discrete devices able to withstand high temperatures is the proper passivation of the devices [137].
- SiC device modelling: The ability to develop and validate accurate device models using modern computer simulation software programs is essential. Thus, users need to be able to simulate their own circuits and design the system with the SiC devices.
- SiC packaging: The packaging of SiC devices has been mostly based on a wire bonding approach on a ceramic substrate, which is a standard method to form interconnects for multichip modules (MCMs), due to its ease of use and relatively lower cost. However, this packaging method has indicated that it is a technical barrier in moving to a higher-performance system enabling operation at high temperatures due to its inherent limitations [138].
- SiC high-speed switching challenges: Although SiC devices are superior in high switching performance compared to their Si counterparts, special consideration needs to be given to fully benefit from their fast-switching feature. The fast-switching transients lead to some issues with the device and package internal electromagnetic parasitics, which are becoming fundamental barriers to the high-performance switching of SiC power devices, which needs to be fixed [126].

4.4. GaN Technology

The GaN devices are among the promising power semiconductor materials that have been used in several power applications such as EV battery chargers, satellite communications, lighting systems, PV inverters, radars, and broadband applications [139,140]. GaN devices have several superior characteristics that make these power devices more attractive for power electronic converters than the conventional Si devices such as a high breakdown tolerance, lower on-resistance, faster switching speeds, and enhanced thermal conductivity [141]. The next generation of semiconductor devices is expected to move steadily towards this type of WBG semiconductor material, which is expected to dominate the power electronics market and will continue to grow with higher voltage ratings. Two types of GaN devices can be found on the market. These types are (i) the depletion mode (d-mode) transistor, known as a normally off switch, and (ii) the enhancement-mode (e-mode) transistor, known as a normally on switch, which can be controlled better than the first type. Currently, there is a strong desire to manufacture GaN devices that can operate

at a voltage level higher than 900 V in order to employ such devices in high-power applications such as WECSs. However, the high cost of manufacturing the devices based on GaN technology is still the main obstacle and requires further research and development efforts. The most-common available GaN devices on the market are currently rated at a range from 100 V to 650 V, and hence, they are suitable for low- and medium-voltage applications. Increasing this voltage range will help with the replacement of Si devices with GaN devices in the power converters and will have positive effects on increasing the switching frequency, decreasing the R_{DS} (on), reducing the switching losses, and improving the thermal conductivity [142,143].

4.4.1. Development of GaN Power Devices

Research efforts have been carried out in the past few decades to develop semiconductor devices based on GaN technology to manufacture transistors (switches) with higher efficiency, which can be used to control HV power systems [144]. Back to the first report issued in 1969, single-crystal GaAs layers using gaseous arsine and epitaxial phosphine from the vapor phase have been reported in [145]. In 2004, a GaN high-electron-mobility transistor (HEMT) based on a depletion-mode (d-mode) transistor was built successfully for the time by the Japanese company Eudyna to be used in radio frequency (RF) applications [146]. Then, the emergence of vertical and lateral GaN HEMT devices has delivered extremely high RF output power densities at the microwave frequency because the aluminium gallium nitride (AlGaN)/GaN interface easily forms a high-electron mobility two-dimensional electron gas (2DEG) and, hence, offers a low on-resistance RDS (on) [147]. The lateral HEMTs may be suitable for low and medium voltage rated up to 650 V and rated current up to 60 A [148]. Figure 17 shows the basic structure of lateral GaN HEMTs [108]. Over years of improvements in the fabrication and optimisation of semiconductor WBG power device technology, the Corporation of Nitrogen announced their GaN-on-Si technology for RF applications. The first normally off GaN HEMT technology was developed and manufactured in 2009 for efficient power conversion to provide more advantages over the normally on GaN HEMT type including a lower $R_{DS\,(on)}$, a lower voltage threshold (VGS), a controllable gate voltage, a higher breakdown voltage, and current collapse suppression [143],[144]. This progress is expected to allow GaN vertical devices to be used in high-voltage and high-current applications [149].

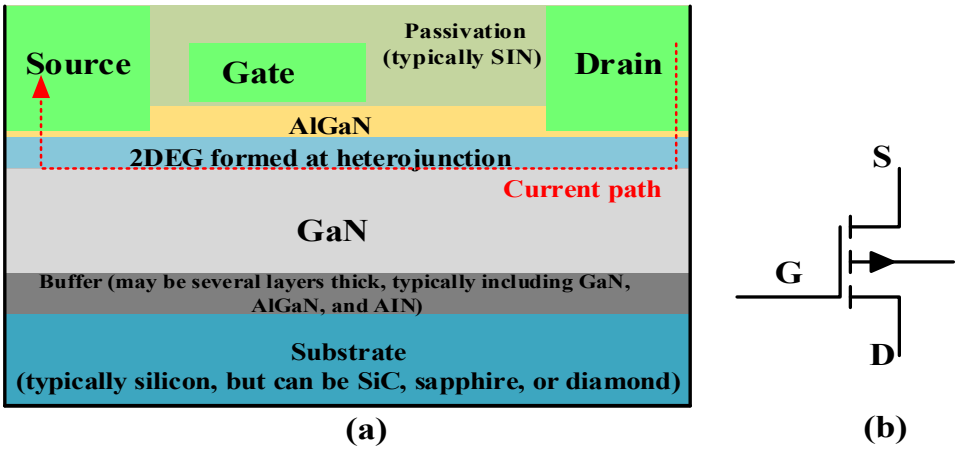

Figure 17. (**a**) Basic structure of lateral GaN HFETs; (**b**) their symbol structure [143].

GaN-on-Si [150] and Schottky diodes [151] both have been suggested as cost-effective alternative technologies for vertical GaN devices with large-scale availability. The first vertical transistor was proposed and demonstrated on six-inch Si substrates in [152]. The vertical transistors are designed for practical use in various converter topologies such as voltage source inverters and buck and boost resonant converters. Liu C. et al., in 2018,

proposed vertical GaN MOSFETs with a freewheeling SBD, as shown in Figure 18. The resultant GaN-on-Si MOSFET-SBD based on enhancement-mode (e-mode) technology has a 3.9 V voltage threshold and an *on/off* ratio of over 10^8, and it optimised the reverse conduction system without any effects for the on-state performance of the SBD integrator. This step marks a great advance for GaN-on-Si vertical devices, which can be used for high-power converter applications [153].

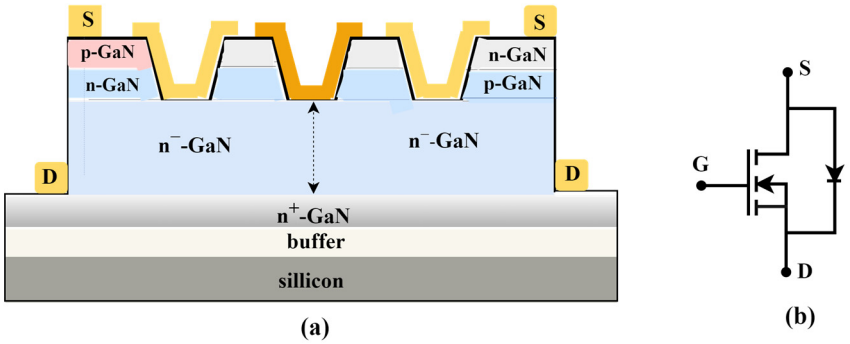

Figure 18. (**a**) Configuration of integrated vertical MOSFET-SBD and (**b**) its symbol structure. Copied with permission from [153].

4.4.2. GaN's Key Challenges

Although the GaN semiconductor devices have outstanding properties, some challenges need to be considered before they can be widely used in different applications. This is due to the lack of bulk GaN source materials, which leads to growing GaN materials on the mismatched substrates of the SiC and Si materials to improve the interconnection parasitics, reduce electromagnetic interference (EMI), and increase the reliability of the devices for high-power applications with acceptable cost. Before designing an electronic power system using power devices based GaN technology, it is really important to understand their features and the associated challenges as discussed below [154,155]:

- Material growth: High-quality materials are the core of GaN-based power devices. Compared to the conventional Si material, the contact mismatch between SiC and sapphire is smaller, and it has higher thermal conductivity, which is a necessary feature for high-power conversion devices [155]. Nevertheless, the practical use of the devices is limited due to the high cost. Despite the large lattice mismatch between GaN and Si, its cost is lower as the lattice mismatch could be attenuated with the buffer layer preface for stress management. Therefore, the Si substrate is still the mainstream material of GaN-based power devices. Furthermore, due to the heterogeneous structure of GaN devices as the power devices, GaN technology is mainly a lateral structure, which makes these devices preferable in the high-frequency field, but also limits their high-power characteristics. At present, the further development and improvement of GaN-based switches by the semiconductor manufacturers have shown that GaN power devices with a rated voltage up to 1200 V will be more suitable for medium and high voltage [156].
- Suppressing the collapse current effect: The effect of the current collapse of the AlGaN/GaN HEMT power devices is one of the major challenges that must be solved to achieve the success of GaN devices in high-power converters. The current collapse effect occurs when a great bias is applied to the drain terminal, where the leakage of the current decays, as shown in Figure 19. The phenomenon of the current collapse effect of GaN devices mainly includes the following [157,158]:
    1. The carrier traps resulting from the deep level centres in the material create the collapse of the current.

2. The polarisation charge modification resulting from the surface effect and the surface state leads to a decrease in the concentration of 2DEG in the conductive AlGaN/GaN channel, which drives the current collapse.
3. The structure of the material and the border of the energy band structure are critical parts because some disturbances will impact the 2DEG and cause current collapse [122]. However, there are some techniques that have been used to suppress the current collapse such as surface passivation treatment [123], the field plate structure [124] and the growth of the P-type cap layer [125].

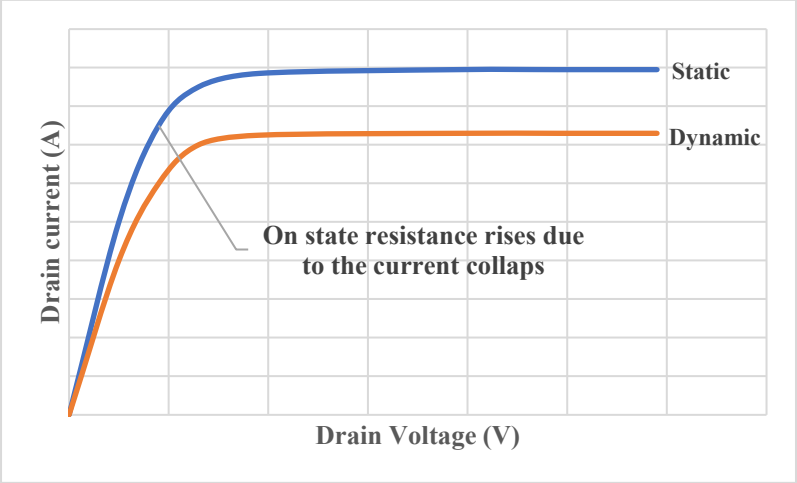

Figure 19. The effect of current collapse on AlGaN/GaN HEMT power device [157].

- Vertical isolation: The vertical isolation is one of the challenges of GaN device, which is affected by the dependence of the conductive substrate potential and drives a back-gating impact. A potential solution for this problem can be implemented by further development of the GaN buffer thickness or by replacing the step-graded buffer of Al-GaN/GaN with a superlattice buffer [159]. Another approach is to use Qromis substrate technology (QSTR) with deep trench isolation and a topical substrate connect [160]. These potential modes help avoid the backdoor effects. However, the GaN-on-Si with an improved buffer may lead to increasing the device's cost compared to the Si technique. On the wafer level, this can be achieved by wafer transfer techniques in a second carrier substrate or by using the remaining frame for selective Si removal with mechanical stabilisation. At the package level, the printed circuit board (PCB) carrier substrate, which is the material that connects the tracks and components that form the basis of a printed circuit board, with embedded GaN-on-Si ICs can be used to remove the Si substrate [161].
- GaN-based complementary metal–oxide semiconductor (CMOS) technology: There have been various demonstrations of GaN-based ICs. These demonstrations are based on the d-mode and e-mode integration of n-type AlGaN/GaN HEMTs. However, these technologies suffer from the static power dissipation and reduced voltage swing at the output terminal, where the GaN power IC technology also allows a p-GaN layer to be used for a p-channel transistor, and the first structure of a p-channel field effect transistor (P-FET) was realised in [162]. Then, both transistors were integrated into a GaN CMOS inverter and published in [163], but this technology also suffers from the lack of high performance, and the challenges of its monolithic integration with e-mode n-FET devices are the main roadblocks towards achieving a better technology since the integration of GaN p-FETs with n-FET devices is more expensive. Thus, the design of a more-efficient gate driver circuit may be required, and further peripherals are feasible through this extension [164].

- The possibility of the combination of vertical and lateral device technologies: During the last two decades, power devices based on GaN technology have been reasonably improved by delivering commercial transistor types with operating voltages up to 1200 V such as a novel normally off GaN vertical transistor with submicron fin-shaped channels, which was published in [165]. In this device, the technology needs only n-GaN layers with no request for epitaxial regrowth or p-GaN layers and specific $R_{DS\,(on)}$ 0.2 mΩ, where the flow of the electrons from the source to the drain modified by the gate deposited on the sidewalls of a narrow sub-micron fin as the width and doping of the fin determines the threshold voltage of the device. A breakdown voltage over 1200 V has been demonstrated with a high on current up to 25 KA/cm^2 and a low off current at 1200 V below 10^{-4} A/cm^2, which makes rendering an excellent Baliga's figure of merit up to 7.2 GW/cm^2. The vertical and lateral GaN devices have the potential to serve a large range of power-switching applications. Thus, the integration of the lateral and vertical structures with a focus on the features of both technologies may lead to an improved transistor with better performance [166]. However, there are some challenges that need attention during the integration of both devices such as the substrate, P-GaN ion implantation, where ion implantation is a common method for Si doping of SiC, channel mobility, and e-mode operation [164,167].

4.5. Hybrid Device Technology

Since the MMC topology requires high-frequency switching devices to improve the system performance and reduce the power losses, WBG-based devices with their distinct characteristics are considered as a promising solution for many power applications, and they have the potential to improve power converter performance in terms of efficiency and low switching and conduction power losses [168]. However, replacing Si-based switches with pure SiC or GaN devices could be more expensive than using the traditional IGBTs and MOSFETs, which is the main reason behind restricting the use of these devices in some applications [169]. Recently, the concept of using hybrid power switches to design power converter topologies in order to control the flow of power has gained more interest for WBG devices. WBG semiconductor power device architectures have moved to higher switching frequencies, as they can improve the power system reliability by reducing the size, weight, and cost. Thus, research efforts have been conducted to show some new ways of combining the existing discrete Si and SiC power devices into one device that has superior performance and can be used in power electronic applications. Furthermore, integrating either SiC or GaN power devices with Si IGBT power switches into any of the SM structures can obtain the benefits of both technologies in one power system and ensure voltage stability at a lower cost [26,170].

Moreover, semiconductor power devices are the key components of many power application systems such as power-converter topologies, gate drivers, and voltage-clamping circuits. Power converters are usually designed based on Si IGBT and MOSFET switches because they are characterised by overcurrent and short-circuit capability [169]. A new hybrid modular multilevel converter (MMC) topology was published in [171], where the proposed MMC model employed a low-switching-loss SiC MOSFET for the HB SMs in the upper arm and used the conventional Si IGBT low-cost feature for the HB SMs in the lower arm, as shown in Figure 20. The resultant hybrid MMC topology has led to several benefits including improving the performance and optimising the cost. Another approach was suggested in [172] employing Si/SiC hybrid devices, where the topology was based on SiC SMs used in the upper arm FB SMs and Si devices used in the lower arm SMs to improve the MMC operation, as shown in Figure 21. The hybrid MMC has demonstrated an efficiency improvement of 16.3% with a 41.0% lower device cost compared with the pure SiC FB SMs. Furthermore, the Si/SiC-hybrid-system (HyS)-switch-based solid-state circuit breaker (SSCB) was proposed in [173], where the switching model combines the Si IGBT and SiC MOSFET, which results in a Si/SiC HyS switch, which can be used for DC applications. It has also been used in the design of a three-level active neutral-point-

clamped (3L-ANPC) converter in [81]. Figure 22 shows the proposed 3L-ANPC inverter topology based on the Si/SiC HyS switch, which allows better efficiency and power capacity and a lower device cost.

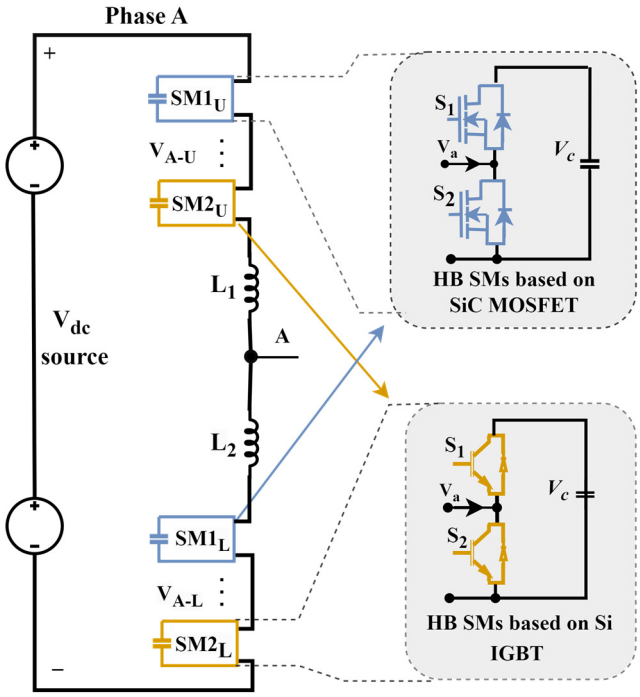

Figure 20. Single-phase MMC topology based on a hybrid Si IGBT and SiC MOSFET SM. Copied with permission from [171].

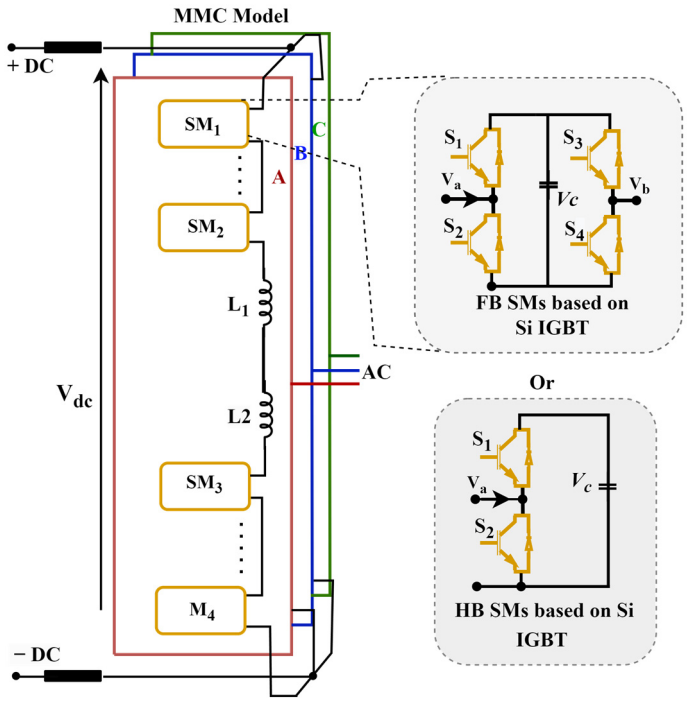

Figure 21. MMC topology based on a Si/SiC HyS FB SMs. Copied with permission from [172].

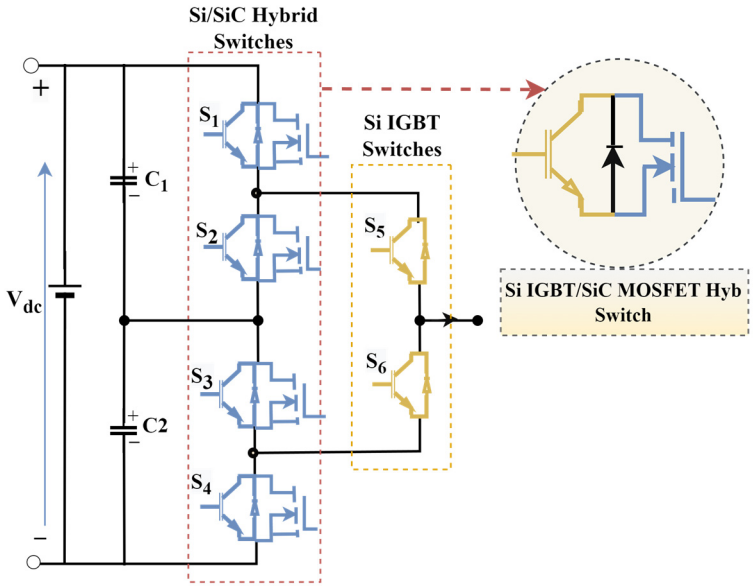

Figure 22. 3L-ANPC inverter topology based on the Si/SiC HyS switch. Copied with permission from [174].

5. Comparison of Si with WBG-Based Devices

This section presents a comparison between the main semiconductor power device technologies that have been used in several power-converter applications such as the MMC topology. Figure 23 shows the performance comparison between the conventional Si and WBG devices' characteristics. For the wind-energy-conversion systems, the majority of power converter topologies are based on Si IGBT and MOSFET devices as these power switches have become the preferred solution for power transmission systems in many power applications because they can handle higher voltages up to 6.5 kv and they can operate at junction temperature up to 150 °C at an affordable cost [131]. On the other hand, devices based on Si technology have some shortcomings, which were mentioned in Section 1 [175]. Due to the advent of more-efficient power semiconductor devices based on SiC and GaN WBG technology, it might be possible to resolve the challenges associated with the traditional Si-based devices. WBG-based devices have demonstrated a higher switching speed capability, greater efficiency, high power density, and smaller size compared to Si technology, which results in the possibility of replacing the pure Si devices with pure or hybrid WBG semiconductor devices in power converter topologies [176]. From the comparison in Figure 23, it is evident that the SiC- and GaN-based devices have superior characteristics such as lower on-state resistance, high switching frequency, a shorter turn off time, and less conduction loss. The material properties' comparison is summarised as follows [177]:

- WBG materials have the potential of operating at higher temperatures up to 300 °C due to their energy gap width of three-times that of the Si material, which has a maximum temperature around 150 °C.
- The WBG materials' critical breakdown voltage is around ten-times that of the Si material. Therefore, the electric breakdown voltage strength is greater in SiC and GaN materials than Si. Additionally, WBG-based devices usually have a lower resistance value, which makes these devices have less conduction loss.
- WBG materials have higher electron mobility compared with the Si-based material, which means the speed of electrons under an electric field is higher, indicating less electrical *on* resistance.

- WBG materials have a higher switching frequency (speed), which means switching between the *on* and *of* states is higher for WBG technology compared to the Si-based material.
- In terms of higher thermal conductivity, SiC-based devices have a thermal conductivity three-times greater than Si-based power switches, which means the thermal resistance is lower and the junction temperature rises at a lower rate compared to Si devices.

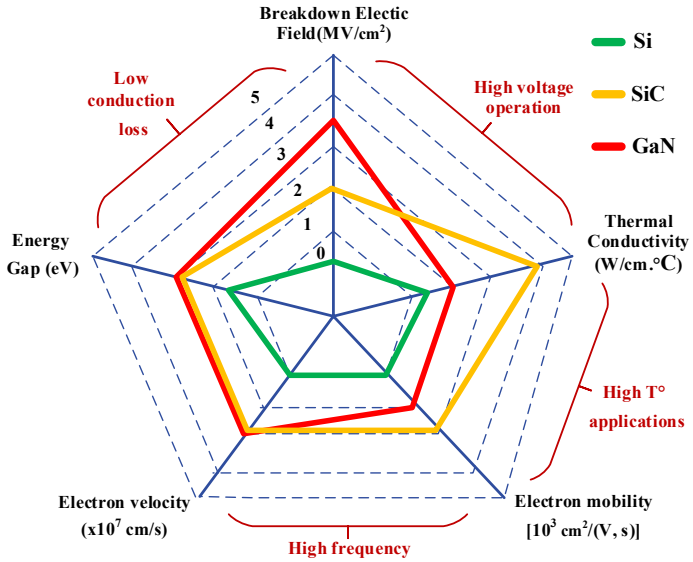

Figure 23. Comparison of Si and WBG semiconductor material properties [143].

5.1. Si IGBT and SiC MOSFET Hybrid Technology

The high cost of devices based on WBG technology is the main obstacle to using these devices in some power applications such as WECSs. Therefore, hybrid switch technology may be the ideal solution for many power applications, among which are wind systems. The technology of Si/SiC hybrid devices is a combination of Si IGBTs and SiC MOSFETs in parallel, designed as one switch and expected to be an alternative to a single Si IGBT or SiC MOSFET device to achieve a high-power quality while reducing power loss and cost [178]. This technique combines the benefits of both material-based devices, which helps to reduce the switching losses and improve the converter performance with an affordable cost [129]. Figure 24 shows the power loss comparison between Si, SiC, and Si/SiC HyS devices that have been used for a three-phase NPC inverter. As expected, the loss reduction reached 70% when pure SiC devices were used, and in the HyS model, the loss reduction reached 45% compared to the pure Si-based model. Thus, the use of HyS-based devices is considered as a satisfactory compromise for power converter topologies [179,180].

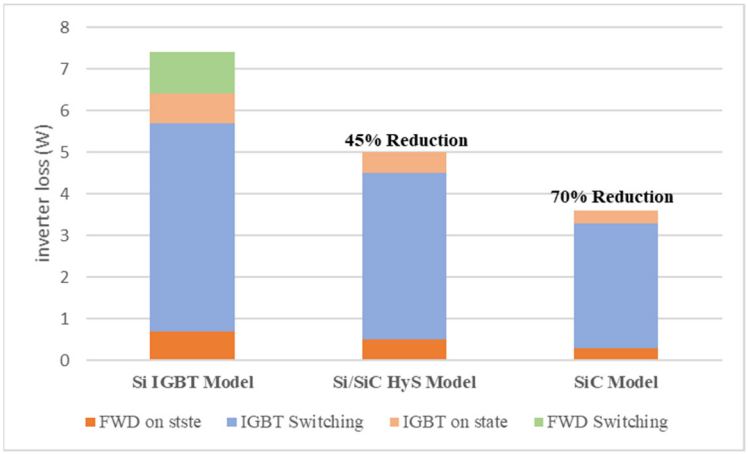

Figure 24. Comparison of total NPC inverter power loss based on Si, SiC, and HyS modules. Copied with permission from [81].

Thereafter, a solid-state circuit breaker (SSCB) based on a Si IGBT and SiC MOSFET HyS was proposed for HVDC power applications [173]. An HyS switch has been used for an NPC inverter, shown in Figure 22 [81]. Figure 25 illustrates the conduction characteristic curve for the three semiconductor device types that use a pure Si IGBT, pure SiC MOSFET, and Si/SiC HyS when they were experimentally tested. Two 1200 V, 75 A Si IGBTs were selected from Infineon® company and connected in parallel, while two 1200 V, 74 A SiC MOSFETs were selected from Wolfspeed® company. The switches from both technologies were combined in a Si/SiC HyS, where the device power ratings of the three solutions was 1200 V, 150 A. The results showed that the Si/SiC HyS model had lower conduction loss than the pure Si IGBTs model, while it had a higher conduction loss than the pure SiC MOSFET model. The pure SiC MOSFET demonstrated less conduction loss compared with the pure Si IGBT and Si/SiC HyS technologies [173].

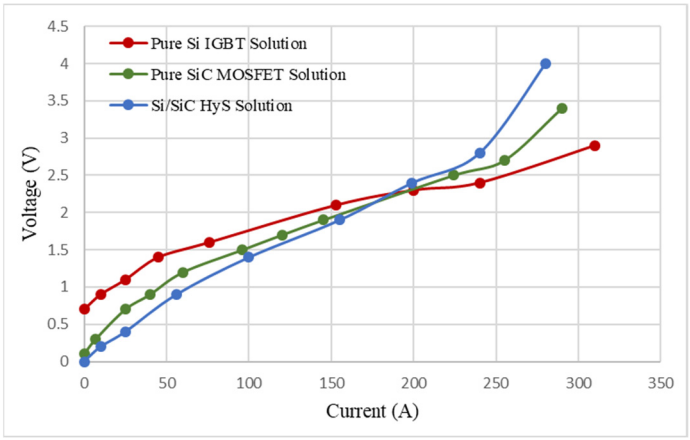

Figure 25. Conduction characteristic curve of Si IGBT, SiC MOSFET, and Si/SiC HyS models. Copied with permission from [173].

A cost comparison between three types of semiconductors was considered in the experiments in [173], using a pure Si IGBT, which is the least expensive power device, a pure SiC MOSFET and a Si/SiC HyS device. Figure 26 shows that using pure SiC MOSFET technology is more expensive than pure Si IGBT devices, while the Si/SiC hybrid device had about a 15% lower cost compared with the pure SiC MOSFET device.

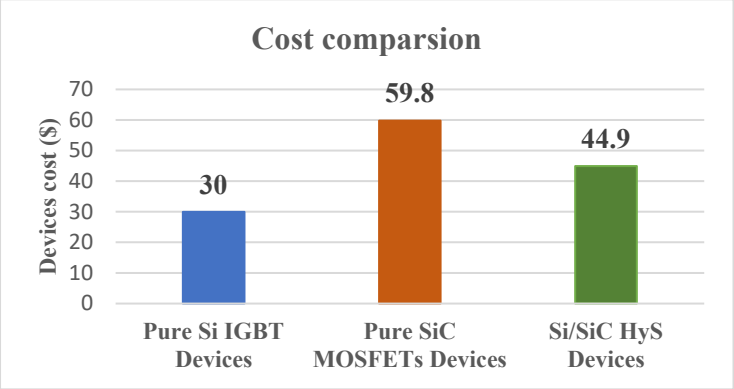

Figure 26. The cost comparison of some semiconductor devices. Copied with permission from [173].

5.2. Integration of Si Devices with GaN HEMT Technology

Basically, GaN HEMT technology combines the low-voltage normally off and high-voltage normally on GaN HFET with a Si MOSFET into a completely new channel to achieve normally off operation **with** a voltage level up to 1200 V [115]. It has similar characteristics to the SiC MOSFET such as outstanding conduction temperature operating capabilities with a fast switching speed [181]. However, the high cost and low voltage rating hinders this type to replace the pure Si IGBT completely. Therefore, instead of utilising pure GaN semiconductor devices, hybrid technologies such as a GaN HEMT/Si IGBT HyS device or a GaN HEMT/SiC MOSFET have been designed to gain the full benefit of the characteristics of both devices. The resultant devices can be the potential solution to resolving the aforementioned challenges of power systems. Nevertheless, the integration of GaN devices with Si technology has not widely matured so far considering some of the challenges that may be faced in the design of such hybrid semiconductor switches, such as the impact of parasitics and the high cost of GaN-based devices being about ~5-times of Si devices [182]. GaN devices have a limited power rating of 650 V, 60 A, and GaN/Si HyS technology usually requires a different gate driver [180].

Figure 27 shows the technology combining the GaN HEMT/Si MOSFET in a HyS device, which was proposed in [183]. The GaN/Si HyS switch is designed based on two GaN HEMTs merged in parallel with Si MOSFETs. The switch model was fully estimated from the switching transient process to the steady state performance and demonstrated excellent benefits for zero-voltage-switching (ZVS) power applications, where the dead-band loss is reduced by the Si body diode. However, not all current passes through the Si body diode during the dead band due to the Si device's parasitic elements, which affects the performance of the body diode and causes reverse recovery loss. Despite the different gate control techniques, which depend on the type of power devices, all such HyS structures must follow a certain rule, where the Si MOSFET must be turned off earlier than the GaN HEMT to achieve a ZVS turn-off of the Si MOSFET and guarantee the use of the excellent switching characteristics for both the GaN HEMT and Si MOSFET to improve the overall switching loss of the system.

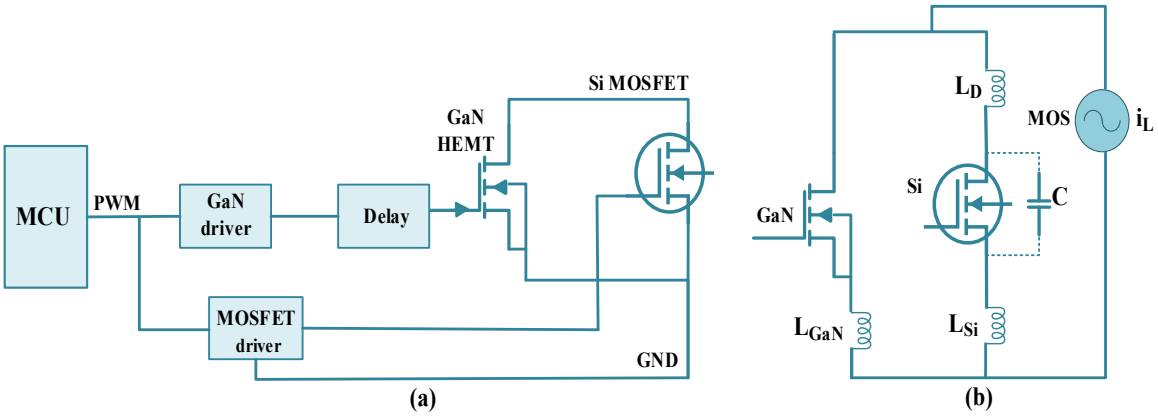

Figure 27. (**a**) Schematic diagram of a GaN/Si HyS switch unit; (**b**) GaN+Si hybrid module equivalent circuit. Copied with permission from [183].

6. Summary

Semiconductor power devices play a major role in many power application systems, especially in the design of power converter topologies for AC–DC rectifiers and DC–AC inverters, which are used for either changing the voltage level or the frequency between the input and output terminals in order to deliver the energy from the supply to the load via a reliable system. The operation of inverter models is based on the switching sequence and the frequency of the power transistors by using a pulse-modulated signal to drive their gate. However, the bulk portion of power losses are caused by the power semiconductor switches, which limit the performance of power converters in terms of efficiency and power density [184,185].

The growing requirements of WECSs may push the limit for the use of multi-level power converters based on Si devices and moving towards the performance of WBG-based devices due to their advantages such as the high operation voltage, high switching frequency, and low loss [186]. Presently, the MMC is the most-widely used power converter topology in wind systems, especially in HVDC applications due to its several advantages. However, the major technical challenge of the MMC model is that it requires a large number of SMs, which use power switches connected in parallel with a capacitor, where the balancing of the voltage capacitors is the main requirement in the MMC topology, and this can be achieved by measuring the instantaneous capacitor voltage at all the SMs to balance the converter system. Thus, the number of power components leads to an increased control complexity, high power loss, and failure possibilities [146].

Power converter designers for WECSs are constantly aiming at achieving high performance and reliability at lower power loss and cost. The choice of a suitable modulation or control system for the MMC topology such as the MPC technique will play an important role in eliminating the harmonics and ensuring system stability. Most power converter topologies including MMCs are designed based on Si device technology such as MOSFET and IGBT switches, which have been widely used due to their performance, wide availability, and affordability [114]. Recently, the development of WBG devices such as SiC- and GaN-based switches has gained wide acceptance in energy conversion applications, and they have the potential to be integrated into the HVDC applications in the near future due to their premium switching characteristics compared to Si [122]. In addition, several companies currently are producing commercially available MOSFETs, power SiC Schottky diodes, and modules. For example, Wolfspeed® company offers power devices such as SiC Schottky diodes with ratings of 650 V to 1700 V and current from 1 A to 50 A, SiC MOSFETs with ratings of 900 V to 1700 V, and SiC power modules with ratings from 1200 V to 1700 V and current up to 90 A [171]. GaN System® company also offers many GaN devices with a voltage rating of around 650 V and a current rating up to 90 A,

where the type is a cascode GaN FET device available with a voltage level up to 1200 V and up to 60 A [165,187].

The manufacturing and design of devices based on WBG technologies are developing and will become available with different rated voltages, which may attract many researchers in the field of power applications to use these devices as alternative solutions. Presently, the use of SiC MOSFETs or GaN HEMTs instead of conventional Si IGBTs for the MMC topology can certainly improve the system's efficiency and reduce the power loss. However, the design of an MMC topology that is completely based on pure SiC MOSFETs or pure GaN devices would be very expensive compared to those based on Si devices. As reported in the literature, the cost of WBG devices is still 3-8-times higher than the conventional Si counterparts [115]. In addition, the global power semiconductor market is expected to reach over *USD* 50×10^9 by the end of 2025 [188]. On the other hand, the solution of hybrid semiconductor technologies such as SiC MOSFETs/Si IGBTs and GaN HEMTs with Si IGBTs or MOSFETs had shown a higher performance with an affordable cost compared to the pure devices based on WBG technology. HyS devices are expected to play a major role in WECSs by merging these devices into the MMC topology as an alternative solution to reduce the total switching and conduction losses, as well as to reduce the cost and increase the system efficiency [189,190]:

- Devices based on WBG power semiconductors typically have a thinner body and lower resistance $R_{DS\,(on)}$, where the lower resistance value results in a lower temperature and, hence, lower conduction losses, where replacing conventional devices in the MMC topology with devices that have a lower $R_{DS\,(on)}$ will result in less heat and lower power losses [186].
- The power devices based on WBG materials have a higher breakdown voltage due to their high electric breakdown field. For example, the Si Schottky diodes are available at rated voltages of less than 300 V, while the commercial SiC Schottky diodes are usually available with rated voltages up to 600 V.
- The market for WBG-based power semiconductors offers switches with different voltage levels such as SiC devices that are available at rated voltages up to 1700 V and current ratings of 80 A. GaN devices have a rated voltage up to 1200 V and current up to 90 A, allowing these devices to be used in the MMC topology for WECSs [171,179].
- WBG power devices have a high thermal conductivity, as shown in Table 3 (1.5 W/cm-K for Si, 4.9 W/cm-K for SiC, and 2.3 W/cmK for GaN). Consequently, power devices based on WBG technology have lower junction thermal resistance (Rth-jc). This means that removing the heat from the device is easier, which results in a slowdown in the increase of the device temperature [191].
- Semiconductor power devices based on WBG technology can operate at a high temperature as SiC devices can operate at high temperatures up to 300 °C, while GaN devices can operate at temperatures up to 225 °C. This is to be compared with the Si devices, where the maximum operating temperature is only up to 150 °C, where devices that have the ability to operate at higher temperatures can be beneficial by reducing switch failures in the MMC system.
- Power devices based on WBG technology are more reliable since they have slightly different forward and reverse characteristics with temperature and time.
- Power devices based on WBG materials have a superior recovery property with lower current reverse recovery. This leads to a reduction in switching losses and EMI, and there is less need for snubber circuits.
- Semiconductor power devices based on WBG materials can operate at higher frequencies (>20 kHz). These devices with fast switching will be useful for the MMC topology.

7. Conclusions

With the rapid growth in the capacity of the WECSs across the world, the impacts of voltage stability and efficiency issues caused by the connection to the power grid have increased, making the demand for an efficient power conversion system an important goal for many researchers. In the power converter stage, semiconductor power devices play a major role in the development of power converter topologies for low-, medium-, and high-power applications. Several converter topologies have been developed for integrating the wind turbines into the power grid including the MMC topology, which has drawn considerable attention due to its high reliability, scalability, and high-quality AC/DC output waveforms. However, the MMC-based wind system still suffers from several problems such as increasing the number of semiconductor components in the SMs and the dependence on Si technology, which increases the heat and power loss, raises the possibility of failures, and increases the current harmonics due to operating at low switching frequencies.

This paper presented a detailed review of semiconductor power devices based on WBG technology in terms of the devices' development, characteristics, and associated challenges. Furthermore, the paper displayed a brief summary of MMC circuit topologies that have been designed based on Si devices, as well as presented their modulation techniques. The semiconductor power device market has matured and grown significantly, and the new devices such as the SiC- and GaN-based have become more attractive to many researchers due to their superior properties such as high switching ability, low switching losses, and the capability of operating at higher temperatures up to 300 °C compared to the Si-based devices, which have a maximum temperature of around 150 °C. Currently, there are many companies producing commercially available MOSFETs, Schottky diodes, and modules that are based on WBG materials. For example, Wolfspeed® company offers SiC MOSFETs with a voltage rating up to 1700 V and current up to 80 A, as well as GaN devices, which are available with a voltage rating up to 650 V and a current rating of 90 A. Thus, the rapid development of power devices based on WBG technology is pushing these switches to be an alternative solution for the MMC topology, replacing the traditional Si IGBTs and MOSFETs. However, the high cost of WBG devices remains the main obstacle limiting the integration of these devices into WECSs. On the other hand, the use of hybrid power devices such as Si/SiC or Si/GaN HEMT technologies are expected to be the ideal solution for the MMC topology. Additionally, the HyS devices have demonstrated a great performance with about a 15% lower cost compared with the pure SiC-based devices because the cost depends on the characteristics of both devices that could be used in the HyS technology. As a conclusion, the development of the MMC SM structures based on HyS switches as a new suggestion is being researched, aiming at reducing the cost, the total footprint, and the energy loss and improving the wind system's performance.

Author Contributions: Conceptualisation, A.A.; methodology, A.A. and A.D.; software, A.A. and A.D.; validation, A.A.; formal analysis, A.A.; investigation, A.D.; resources, A.A. and A.D.; data curation, A.A. and A.D.; writing—original draft, A.A.; writing—review and editing, A.A. and A.D.; visualisation, A.A. and A.D.; supervision, A.D.; project administration, A.D.; funding acquisition, A.D. All authors have read and agreed to the published version of the manuscript.

Funding: This research received no external funding.

Data Availability Statement: Not applicable.

Acknowledgments: The authors are sincerely grateful to the financial sponsor for making this research possible.

Conflicts of Interest: The authors declare no conflict of interest.

References

1. Wang, S.; Wang, S. Impacts of wind energy on environment: A review. *Renew. Sustain. Energy Rev.* **2015**, *49*, 437–443. https://doi.org/10.1016/j.rser.2015.04.137.

2. Hossain, M.J.; Pota, H.R.; Mahmud, A.; Ramos, R.A. Investigation of the Impacts of Large-Scale Wind Power Penetration on the Angle and Voltage Stability of Power Systems. *IEEE Syst. J.* **2012**, *6*, 76–84. https://doi.org/10.1109/jsyst.2011.2162991.
3. BP Statistical Review of World Energy Globally Consistent Data on World Energy Markets and Authoritative Publications in the Field of Energy. *BP Energy Outlook* **2021**, *70*, 72.
4. Jung, C.; Schindler, D. Development of onshore wind turbine fleet counteracts climate change-induced reduction in global capacity factor. *Nat. Energy* **2022**, *7*, 608–619. https://doi.org/10.1038/s41560-022-01056-z.
5. Global Wind Energy Council. *Global Wind Report 2022*; GWEC: Brussels, Belgium, 2022; p. 75.
6. Global Wind Organisation. *Global Wind Energy Council Global Wind Workforce Outlook 2021–2025*; Global Wind Organisation: København K, Denmark, 2021.
7. Niu, T.; Wang, J.; Du, P.; Yang, W. WPFSAD: Wind Power Forecasting System Integrating Dual-Stage Attention and Deep Learning. *IEEE Trans. Ind. Informatics* **2023**, 1–12. https://doi.org/10.1109/tii.2023.3245196.
8. Zhang, B.; Wang, S. An Overview of Wide Bandgap Power Semiconductor Device Packaging Techniques for EMI Reduction. In Proceedings of the 2018 IEEE Symposium on Electromagnetic Compatibility, Signal Integrity and Power Integrity (EMC, SI & PI), Long Beach, CA, USA, 30 July–3 August 2018; pp. 297–301. https://doi.org/10.1109/emcsi.2018.8495171.
9. Devashish; Thakur, A.; Panigrahi, S.; Behera, R.R. A Review on Wind Energy Conversion System and Enabling Technology. In Proceedings of the International Conference on Electrical Power and Energy Systems, ICEPES, Bhopal, India, 14–16 December 2016; 2017; pp. 527–532.
10. Darwish, A.; Massoud, A.; Holliday, D.; Ahmed, S.; Williams, B. Generation, performance evaluation and control design of single-phase differential-mode buck–boost current-source inverters. *IET Renew. Power Gener.* **2016**, *10*, 916–927. https://doi.org/10.1049/iet-rpg.2015.0343.
11. Darwish, A.; Elserougi, A.; Abdel-Khalik, A.S.; Ahmed, S.; Massoud, A.; Holliday, D.; Williams, B.W. A single-stage three-phase DC/AC inverter based on Cuk converter for PV application. In Proceedings of the 2013 7th IEEE GCC Conference and Exhibition (GCC), Doha, Qatar, 17–20 November 2013; pp. 384–389. https://doi.org/10.1109/ieeegcc.2013.6705809.
12. Zhang, G.; Li, Z.; Zhang, B.; Halang, W.A. Power electronics converters: Past, present and future. *Renew. Sustain. Energy Rev.* **2018**, *81*, 2028–2044. https://doi.org/10.1016/j.rser.2017.05.290.
13. Nabae, A.; Takahashi, I.; Akagi, H. A New Neutral-Point-Clamped PWM Inverter. *IEEE Trans. Ind. Appl.* **1981**, *IA-17*, 518–523. https://doi.org/10.1109/tia.1981.4503992.
14. Meynard, T.A.; Foch, H. Multi-level conversion: High voltage choppers and voltage-source inverters. In Proceedings of the PESC'92 Record, 23rd Annual IEEE Power Electronics Specialists Conference, Toledo, Spain, 29 June–3 July 1992; pp. 397–403. https://doi.org/10.1109/pesc.1992.254717.
15. Babaei, E.; Laali, S.; Alilu, S. Cascaded Multilevel Inverter with Series Connection of Novel H-Bridge Basic Units. *IEEE Trans. Ind. Electron.* **2014**, *61*, 6664–6671. https://doi.org/10.1109/tie.2014.2316264.
16. Pwm, M.L. Operation of a Seven-Level T-Type Active Neutral-Point-Clamped Converter With. *IEEE Trans. Ind. Electron.* **2021**, *68*, 10970–10981.
17. Akagi, H. Multilevel Converters: Fundamental Circuits and Systems. *Proc. IEEE* **2017**, *105*, 2048–2065. https://doi.org/10.1109/jproc.2017.2682105.
18. Darwish, A.; Holliday, D.; Finney, S. Operation and control design of an input conversion scheme for offshore DC wind systems. *IET Power Electron.* **2017**, *10*, 2092–2103. https://doi.org/10.1049/iet-pel.2016.0885.
19. Badawy, A.D. Current Source DC-DC and DC-AC Converters with Continuous Energy Flow By. Ph.D. Thesis, University of Strathclyde, Glasgow, UK, 2015.
20. Wang, B. Review of Power Semiconductor Device Reliability for Power Converters. *CPSS Trans. Power Electron. Appl.* **2017**, *2*, 101–117. https://doi.org/10.24295/cpsstpea.2017.00011.
21. Dekka, A.; Ramezani, A.; Ounie, S.; Narimani, M. A New 5–Level Voltage Source Inverter. In Proceedings of the 2019 IEEE Applied Power Electronics Conference and Exposition (APEC), Anaheim, CA, USA, 17–21 March 2019; pp. 2511–2515. https://doi.org/10.1109/apec.2019.8721809.
22. Blaabjerg, F.; Ma, K.; Yang, Y. Power electronics-The key technology for Renewable Energy Systems. In Proceedings of the 2015 International Conference on Renewable Energy Research and Applications (ICRERA), Palermo, Italy, 22–25 November 2015; pp. 1–11. https://doi.org/10.1109/ever.2014.6844159.
23. Elasser, A.; Chow, T. Silicon carbide benefits and advantages for power electronics circuits and systems. *Proc. IEEE* **2002**, *90*, 969–986. https://doi.org/10.1109/jproc.2002.1021562.
24. She, X.; Huang, A.Q.; Lucia, O.; Ozpineci, B. Review of Silicon Carbide Power Devices and Their Applications. *IEEE Trans. Ind. Electron.* **2017**, *64*, 8193–8205. https://doi.org/10.1109/tie.2017.2652401.
25. Blaabjerg, F.; Chen, Z.; Kjaer, S.B. Power Electronics as Efficient Interface in Dispersed Power Generation Systems. *IEEE Trans. Power Electron.* **2004**, *19*, 1184–1194. https://doi.org/10.1109/tpel.2004.833453.
26. Millan, J.; Godignon, P.; Perpina, X.; Perez-Tomas, A.; Rebollo, J. A Survey of Wide Bandgap Power Semiconductor Devices. *IEEE Trans. Power Electron.* **2014**, *29*, 2155–2163. https://doi.org/10.1109/tpel.2013.2268900.
27. Yuan, X.; Laird, I.D.; Walder, S. Opportunities, Challenges, and Potential Solutions in the Application of Fast-Switching SiC Power Devices and Converters. *IEEE Trans. Power Electron.* **2021**, *36*, 3925–3945. https://doi.org/10.1109/tpel.2020.3024862.
28. Shenai, K. High-Density Power Conversion and Wide-Bandgap Semiconductor Power Electronics Switching Devices. *Proc. IEEE* **2019**, *107*, 2308–2326.

29. Tang, Z.; Yang, Y.; Blaabjerg, F. Power electronics-the enabling technology for renewable energy integration. *CSEE J. Power Energy Syst.* **2022**, *8*, 39–52. https://doi.org/10.17775/cseejpes.2021.02850.
30. Yuan, X.; Wang, J.; Laird, I.; Zhou, W. Wide-Bandgap Device Enabled Multilevel Converters with Simplified Structures and Capacitor Voltage Balancing Capability. *IEEE Open J. Power Electron.* **2021**, *2*, 401–410. https://doi.org/10.1109/ojpel.2021.3094713.
31. Gajewski, D.A.; Hull, B.; Lichtenwalner, D.J.; Ryu, S.-H.; Bonelli, E.; Mustain, H.; Wang, G.; Allen, S.T.; Palmour, J.W. SiC power device reliability. In Proceedings of the 2016 IEEE International Integrated Reliability Workshop (IIRW), South Lake Tahoe, CA, USA, 9–13 October 2016; pp. 29–34. https://doi.org/10.1109/iirw.2016.7904895.
32. Ballestín-Fuertes, J.; Muñoz-Cruzado-Alba, J.; Sanz-Osorio, J.F.; Laporta-Puyal, E. Role of Wide Bandgap Materials in Power Electronics for Smart Grids Applications. *Electronics* **2021**, *10*, 677. https://doi.org/10.3390/electronics10060677.
33. Blaabjerg, F.; Ma, K. Future on Power Electronics for Wind Turbine Systems. *IEEE J. Emerg. Sel. Top. Power Electron.* **2013**, *1*, 139–152. https://doi.org/10.1109/jestpe.2013.2275978.
34. Piriienko, S.; Neuburger, M.; Ammann, U.; Balakhontsev, A.; Thrimawithana, D.J.; Cheng, P.-W. Evaluation of the Small-Scale Wind Turbine Converter's Efficiency Built with Various Types of Semiconducting Devices. In Proceedings of the 2018 IEEE 3rd International Conference on Intelligent Energy and Power Systems (IEPS), Kharkiv, Ukraine, 10–14 September 2018; pp. 166–171. https://doi.org/10.1109/ieps.2018.8559517.
35. Akhtar, I.; Kirmani, S.; Jameel, M. Reliability Assessment of Power System Considering the Impact of Renewable Energy Sources Integration Into Grid With Advanced Intelligent Strategies. *IEEE Access* **2021**, *9*, 32485–32497. https://doi.org/10.1109/access.2021.3060892.
36. Jamil, M.; Gupta, R.; Singh, M. A review of power converter topology used with PMSG based wind power generation. In Proceedings of the 2012 IEEE Fifth Power India Conference, Murthal, India, 19–22 December 2012; pp. 1–6. https://doi.org/10.1109/poweri.2012.6479549.
37. Suresh, V.; Emayavaramban, G.; Amudha, A.; Balachander, K.; Kavitha, D. Modeling, Design and Implementation of a Power Conversion System for WECS by Using Fuzzy Based MPPT. *J. Adv. Res. Dyn. Control Syst.* **2018**, *10*, 1198–1211.
38. Salem, A.A.; ElDesouky, A.A.; Alaboudy, A.H.K. New analytical assessment for fast and complete pre-fault restoration of grid-connected FSWTs with fuzzy-logic pitch-angle controller. *Int. J. Electr. Power Energy Syst.* **2022**, *136*, 107745. https://doi.org/10.1016/j.ijepes.2021.107745.
39. Jing, T.; Maklakov, A.S. A Review of Voltage Source Converters for Energy Applications. In Proceedings of the Ural Conference on Green Energy (UralCon) 2018 International, Chelyabinsk, Russia, 4–6 October 2018; pp. 275–281.
40. Lesnicar, A.; Marquardt, R. An innovative modular multilevel converter topology suitable for a wide power range. In Proceedings of the IEEE Bologna Power Tech Conference Proceedings, Bologna, Italy, 23–26 June 2003; Volume 3, p. 6. https://doi.org/10.1109/ptc.2003.1304403.
41. Siemaszko, D.; Antonopoulos, A.; Ilves, K.; Vasiladiotis, M.; Angquist, L.; Nee, H.-P. Evaluation of control and modulation methods for modular multilevel converters. In Proceedings of the 2010 International Power Electronics Conference-ECCE ASIA-, Sapporo, Japan, 21–24 June 2010; pp. 746–753. https://doi.org/10.1109/ipec.2010.5544609.
42. Debnath, S.; Saeedifard, M. A New Hybrid Modular Multilevel Converter for Grid Connection of Large Wind Turbines. *IEEE Trans. Sustain. Energy* **2013**, *4*, 1051–1064. https://doi.org/10.1109/tste.2013.2266280.
43. Sahoo, A.K.; Otero-De-Leon, R.; Chandrasekaran, V.; Mohan, N. New 3-level submodules for a modular multilevel converter based HVDC system with advanced features. In Proceedings of the IECON 2013—39th Annual Conference of the IEEE Industrial Electronics Society, Vienna, Austria, 10–13 November 2013; pp. 6269–6274. https://doi.org/10.1109/iecon.2013.6700166.
44. Yu, X.; Wei, Y.; Jiang, Q. New submodule circuits for modular multilevel current source converters with DC fault ride through capability. In Proceedings of the 2016 IEEE Applied Power Electronics Conference and Exposition (APEC), Long Beach, CA, USA, 20–24 March 2016; pp. 1468–1474. https://doi.org/10.1109/apec.2016.7468062.
45. Mishra, R.; Agarwal, V. A Novel Four Terminal Integrated Submodule Modular Multilevel Converter. In Proceedings of the 2018 IEEE International Conference on Power Electronics, Drives and Energy Systems (PEDES), Chennai, India, 18–21 December 2018; pp. 1–6. https://doi.org/10.1109/pedes.2018.8707503.
46. Nami, A.; Adabi, J. A new T-type NPC-based submodule for modular multilevel cascaded converters. In Proceedings of the 5th Annual International Power Electronics, Drive Systems and Technologies Conference (PEDSTC 2014), Tehran, Iran, 5–6 February 2014; pp. 137–142. https://doi.org/10.1109/pedstc.2014.6799359.
47. Alesina, A.; Venturini, M. Solid-state power conversion: A Fourier analysis approach to generalized transformer synthesis. *IEEE Trans. Circuits Syst.* **1981**, *28*, 319–330. https://doi.org/10.1109/tcs.1981.1084993.
48. Konstantinou, G.; Pou, J.; Ceballos, S.; Agelidis, V.G. Active Redundant Submodule Configuration in Modular Multilevel Converters. *IEEE Trans. Power Deliv.* **2013**, *28*, 2333–2341. https://doi.org/10.1109/tpwrd.2013.2264950.
49. Lee, J.-H.; Jung, J.-J.; Sul, S.-K. Balancing of Submodule Capacitor Voltage of Hybrid Modular Multilevel Converter Under DC-Bus Voltage Variation of HVDC System. *IEEE Trans. Power Electron.* **2019**, *34*, 10458–10470. https://doi.org/10.1109/tpel.2019.2896336.
50. Hafeez, K.; Khan, S.A.; Van den Bossche, A.; Hasan, Q.U. Circulating Current Reduction in MMC-HVDC System Using Average Model. *Appl. Sci.* **2019**, *9*, 1383. https://doi.org/10.3390/app9071383.
51. Marquardt, R. Modular Multilevel Converter: Impact on Future Applications and Semiconductors. In Proceedings of the Power Electronic Components and their Applications 2017; 7. ETG-Symposium, Bad Nauheim, Germany, 6–7 April 2017; pp. 100–109.

52. Challa, R.V.K.; Mikkili, S.; Bonthagorla, P.K. Modeling, Controlling Approaches, Modulation Schemes, and Applications of Modular Multilevel Converter: Review. *J. Control. Autom. Electr. Syst.* **2023**, *34*, 189–215. https://doi.org/10.1007/s40313-022-00953-8.
53. Ali, S.; Ling, Z.; Tian, K.; Huang, Z. Recent Advancements in Submodule Topologies and Applications of MMC. *IEEE J. Emerg. Sel. Top. Power Electron.* **2021**, *9*, 3407–3435. https://doi.org/10.1109/jestpe.2020.2990689.
54. Deng, F.; Chen, Z. Voltage-Balancing Method for Modular Multilevel Converters Switched at Grid Frequency. *IEEE Trans. Ind. Electron.* **2015**, *62*, 2835–2847. https://doi.org/10.1109/tie.2014.2362881.
55. Deng, F.; Chen, Z. Voltage-Balancing Method for Modular Multilevel Converters Under Phase-Shifted Carrier-Based Pulse-width Modulation. *IEEE Trans. Ind. Electron.* **2015**, *62*, 4158–4169. https://doi.org/10.1109/tie.2014.2388195.
56. Konstantinou, G.; Zhang, J.; Ceballos, S.; Pou, J.; Agelidis, V.G. Comparison and evaluation of sub-module configurations in modular multilevel converters. In Proceedings of the 2015 IEEE 11th International Conference on Power Electronics and Drive Systems, Sydney, NSW, Australia, 9–12 June 2015; pp. 958–963. https://doi.org/10.1109/peds.2015.7203440.
57. Yang, H.; Fan, S.; Dong, Y.; Yang, H.; Li, W.; He, X. Arm Phase-Shift Conducting Modulation for Alternate Arm Multilevel Converter with Half-Bridge Submodules. *IEEE Trans. Power Electron.* **2021**, *36*, 5223–5235. https://doi.org/10.1109/tpel.2020.3030865.
58. Xu, J.; Zhao, P.; Jiang, W.; Ma, W.; Zhao, C. Reliability Analysis and Redundancy Configuration of Hybrid MMCs with DC Fault Blocking Capability. *Proc. CSEE* **2016**, *36*, 953–960. https://doi.org/10.13334/j.0258-8013.pcsee.2016.04.008.
59. Li, X.; Song, Q.; Liu, W.; Zhu, Z.; Xu, S. Experiment on DC-fault Ride Through of MMC Using a Half-Voltage Clamp Submodule. *IEEE J. Emerg. Sel. Top. Power Electron.* **2018**, *6*, 1273–1279. https://doi.org/10.1109/jestpe.2018.2813329.
60. Kim, H.; Kang, J.; Kim, S.; Kim, C.-K.; Hur, K. DC fault protection for modular multilevel converter HVDC using asymmetrical unipolar full-bridge submodule. In Proceedings of the 2015 9th International Conference on Power Electronics and ECCE Asia (ICPE-ECCE Asia), Seoul, Republic of Korea, 1–5 June 2015; pp. 1083–1089. https://doi.org/10.1109/icpe.2015.7167915.
61. Nguyen, T.H.; Lee, D.-C.; Hai, N.T. A novel submodule topology of MMC for blocking DC-fault currents in HVDC transmission systems. In Proceedings of the 2015 9th International Conference on Power Electronics and ECCE Asia, Seoul, Republic of Korea, 1–5 June 2015; pp. 2057–2063.
62. Qin, J.; Saeedifard, M.; Rockhill, A.; Zhou, R. Hybrid Design of Modular Multilevel Converters for HVDC Systems Based on Various Submodule Circuits. *IEEE Trans. Power Deliv.* **2015**, *30*, 385–394. https://doi.org/10.1109/tpwrd.2014.2351794.
63. Tang, Y.; Chen, M.; Ran, L. A compact MMC submodule structure with reduced capacitor size using the stacked switched capacitor architecture. *IEEE Trans. Power Electron.* **2016**, *31*, 6920–6936. https://doi.org/10.1109/tpel.2015.2511189.
64. Marquardt, R. Modular Multilevel Converter: An universal concept for HVDC-Networks and extended DC-Bus-applications. In Proceedings of the 2010 International Power Engineering Conference (IPEC), Sapporo, Japan, 21–24 June 2010; pp. 502–507.
65. Soeiro, T.B.; Kolar, J.W. The New High-Efficiency Hybrid Neutral-Point-Clamped Converter. *IEEE Trans. Ind. Electron.* **2012**, *60*, 1919–1935. https://doi.org/10.1109/tie.2012.2209611.
66. Dekka, A.; Wu, B.; Zargari, N.R.; Fuentes, R.L. Dynamic Voltage Balancing Algorithm for Modular Multilevel Converter: A Unique Solution. *IEEE Trans. Power Electron.* **2016**, *31*, 952–963. https://doi.org/10.1109/tpel.2015.2419881.
67. Ilves, K.; Taffner, F.; Norrga, S.; Antonopoulos, A.; Harnefors, L.; Nee, H.-P. A Submodule Implementation for Parallel Connection of Capacitors in Modular Multilevel Converters. *IEEE Trans. Power Electron.* **2015**, *30*, 3518–3527. https://doi.org/10.1109/tpel.2014.2345460.
68. Nami, A.; Wang, L.; Dijkhuizen, F.; Shukla, A. Five level cross connected cell for cascaded converters. In Proceedings of the 2013 15th European Conference on Power Electronics and Applications (EPE), Lille, France, 2–6 September 2013; pp. 1–9. https://doi.org/10.1109/epe.2013.6631941.
69. Ilves, K.; Bessegato, L.; Harnefors, L.; Norrga, S.; Nee, H.-P. Semi-full-bridge submodule for modular multilevel converters. In Proceedings of the 2015 9th International Conference on Power Electronics and ECCE Asia (ICPE-ECCE Asia), Seoul, Republic of Korea, 1–5 June 2015; pp. 1067–1074. https://doi.org/10.1109/icpe.2015.7167913.
70. Deng, F.; Lü, Y.; Liu, C.; Heng, Q.; Yu, Q.; Zhao, J. Overview on submodule topologies, modeling, modulation, control schemes, fault diagnosis, and tolerant control strategies of modular multilevel converters. *Chin. J. Electr. Eng.* **2020**, *6*, 1–21. https://doi.org/10.23919/cjee.2020.000001.
71. Yadav, A.; Singh, S.N.; Das, S.P. Modular multi-level converter topologies: Present status and key challenges. In Proceedings of the 2017 4th IEEE Uttar Pradesh Section International Conference on Electrical, Computer and Electronics (UPCON), Mathura, India, 26–28 October 2017; pp. 280–288. https://doi.org/10.1109/upcon.2017.8251061.
72. Baker, I.R.H.; Bannister, L.H. Electric Power Converter. U.S. Patent 3 867 643, 18 February 1975; pp. 1–15.
73. Choudhury, S.; Bajaj, M.; Dash, T.; Kamel, S.; Jurado, F. Multilevel Inverter: A Survey on Classical and Advanced Topologies, Control Schemes, Applications to Power System and Future Prospects. *Energies* **2021**, *14*, 5773. https://doi.org/10.3390/en14185773.
74. Ounejjar, Y.; Al-Haddad, K.; Grégoire, L.-A. Packed U Cells Multilevel Converter Topology: Theoretical Study and Experimental Validation. *IEEE Trans. Ind. Electron.* **2011**, *58*, 1294–1306. https://doi.org/10.1109/tie.2010.2050412.
75. Sorto-Ventura, K.-R.; Abarzadeh, M.; Al-Haddad, K.; Dessaint, L.A. 23-level Single DC Source Hybrid PUC (H-PUC) Converter Topology with Reduced Number of Components: Real-Time Implementation With Model Predictive Control. *IEEE Open J. Ind. Electron. Soc.* **2020**, *1*, 127–137. https://doi.org/10.1109/ojies.2020.3007989.

76. Sharifzadeh, M.; Al-Haddad, K. Packed E-Cell (PEC) Converter Topology Operation and Experimental Validation. *IEEE Access* **2019**, *7*, 93049–93061. https://doi.org/10.1109/access.2019.2924009.
77. Babaie, M.; Al-Haddad, K. Boost Packed E-Cell: A Compact Multilevel Converter for Power Quality Ancillary Services. *IEEE Trans. Ind. Appl.* **2023**, *59*, 554–566. https://doi.org/10.1109/tia.2022.3208221.
78. Nilkar, M.; Babaei, E.; Sabahi, M. A new single-phase cascade multilevel inverter topology using four-level cells. In Proceedings of the 20th Iranian Conference on Electrical Engineering (ICEE2012), Tehran, Iran, 15–17 May 2012; pp. 348–353. https://doi.org/10.1109/iraniancee.2012.6292382.
79. Khosroshahi, M.T. Crisscross cascade multilevel inverter with reduction in number of components. *IET Power Electron.* **2014**, *7*, 2914–2924. https://doi.org/10.1049/iet-pel.2013.0541.
80. Darwish, A. Efficient modular multilevel converter based on active-forcedcommutated hybrid packed u-cells for HV networks. *IET Conf. Publ.* **2019**, *2019*, 1–6. https://doi.org/10.1049/cp.2019.0094.
81. Guan, Q.-X.; Li, C.; Zhang, Y.; Wang, S.; Xu, D.D.; Li, W.; Ma, H. An Extremely High Efficient Three-Level Active Neutral-Point-Clamped Converter Comprising SiC and Si Hybrid Power Stages. *IEEE Trans. Power Electron.* **2018**, *33*, 8341–8352. https://doi.org/10.1109/tpel.2017.2784821.
82. Rodriguez, J.; Lai, J.-S.; Peng, F.Z. Multilevel inverters: A survey of topologies, controls, and applications. *IEEE Trans. Ind. Electron.* **2002**, *49*, 724–738. https://doi.org/10.1109/tie.2002.801052.
83. Prabaharan, N.; Palanisamy, K. A comprehensive review on reduced switch multilevel inverter topologies, modulation techniques and applications. *Renew. Sustain. Energy Rev.* **2017**, *76*, 1248–1282. https://doi.org/10.1016/j.rser.2017.03.121.
84. Samuel, P.; Gupta, R.; Chandra, D. Grid Interface of Wind Power with Large Split-Winding Alternator Using Cascaded Multilevel Inverter. *IEEE Trans. Energy Convers.* **2011**, *26*, 299–309. https://doi.org/10.1109/tec.2010.2096538.
85. Tian, Y.; Wickramasinghe, H.R.; Li, Z.; Pou, J.; Konstantinou, G. Review, Classification and Loss Comparison of Modular Multilevel Converter Submodules for HVDC Applications. *Energies* **2022**, *15*, 1985. https://doi.org/10.3390/en15061985.
86. Leon, J.I.; Vazquez, S.; Franquelo, L.G. Multilevel Converters: Control and Modulation Techniques for Their Operation and Industrial Applications. *Proc. IEEE* **2017**, *105*, 2066–2081.
87. Debnath, S.; Qin, J.; Bahrani, B.; Saeedifard, M.; Barbosa, P. Operation, Control, and Applications of the Modular Multilevel Converter: A Review. *IEEE Trans. Power Electron.* **2015**, *30*, 37–53. https://doi.org/10.1109/tpel.2014.2309937.
88. Abdelsalam, A.K.; Massoud, A.; Darwish, A.; Ahmed, S. Simplified generic on-line PWM technique for single phase grid connected current source inverters. In Proceedings of the 2012 Twenty-Seventh Annual IEEE Applied Power Electronics Conference and Exposition (APEC), Orlando, FL, USA, 5–9 February 2012; pp. 1398–1403. https://doi.org/10.1109/apec.2012.6166003.
89. Tolbert, L.; Habetler, T. Novel multilevel inverter carrier-based PWM method. *IEEE Trans. Ind. Appl.* **1999**, *35*, 1098–1107. https://doi.org/10.1109/28.793371.
90. Das, A.; Nademi, H.; Norum, L. A Pulse Width Modulation technique for reducing switching frequency for modular multilevel converter. In Proceedings of the India International Conference on Power Electronics 2010 (IICPE2010), New Delhi, India, 28-30 January 2011; pp. 1–6. https://doi.org/10.1109/iicpe.2011.5728082.
91. Mwinyiwiwa, B.; Wolanski, Z.; Ooi, B.-T. Microprocessor implemented SPWM for multiconverters with phase-shifted triangle carriers. In Proceedings of the IAS '97. Conference Record of the 1997 IEEE Industry Applications Conference Thirty-Second IAS Annual Meeting, New Orleans, LA, USA, 5–9 October 1997; Volume 2, pp. 1542–1549. https://doi.org/10.1109/ias.1997.629058.
92. Vinnakoti, S.; Daki, A.; Indraganti, V.; Srikar, A.S.; Sampath, K. Performance Analysis of MMC with Novel Multi-Carrier Phase Shifted Pulse Width Modulation (MCPS-PWM). In Proceedings of the 2022 International Conference on Computing, Communication and Power Technology (IC3P), Visakhapatnam, India, 7–8 January 2022; pp. 26–31. https://doi.org/10.1109/ic3p52835.2022.00015.
93. Hagiwara, M.; Akagi, H. Control and Experiment of Pulsewidth-Modulated Modular Multilevel Converters. *IEEE Trans. Power Electron.* **2009**, *24*, 1737–1746. https://doi.org/10.1109/tpel.2009.2014236.
94. Hagiwara, M.; Maeda, R.; Akagi, H. Control and Analysis of the Modular Multilevel Cascade Converter Based on Double-Star Chopper-Cells (MMCC-DSCC). *IEEE Trans. Power Electron.* **2011**, *26*, 1649–1658. https://doi.org/10.1109/tpel.2010.2089065.
95. Nguyen, M.H.; Kwak, S. Simplified Indirect Model Predictive Control Method for a Modular Multilevel Converter. *IEEE Access* **2018**, *6*, 62405–62418. https://doi.org/10.1109/access.2018.2876505.
96. Antonopoulos, A.; Ängquist, L.; Nee, H.P. On Dynamics and Voltage Control of the Modular Multilevel Converter. In Proceedings of the 2009 13th European Conference on Power Electronics and Applications, Barcelona, Spain, 8–10 September 2009.
97. Du, S.; Liu, J.; Liu, T. Modulation and Closed-Loop-Based DC Capacitor Voltage Control for MMC With Fundamental Switching Frequency. *IEEE Trans. Power Electron.* **2015**, *30*, 327–338. https://doi.org/10.1109/tpel.2014.2301836.
98. Fatunmbi, R.O.; Okoye, O.O.; Lasabi, O.A.; Davidson, I.E. FPGA implementation of open-loop controller for five-level three phase modular multilevel converter. In Proceedings of the 2017 IEEE AFRICON, Cape Town, South Africa, 18–20 September 2017; pp. 1345–1350. https://doi.org/10.1109/afrcon.2017.8095677.
99. Angquist, L.; Antonopoulos, A.; Siemaszko, D.; Ilves, K.; Vasiladiotis, M.; Nee, H.-P. Open-Loop Control of Modular Multilevel Converters Using Estimation of Stored Energy. *IEEE Trans. Ind. Appl.* **2011**, *47*, 2516–2524. https://doi.org/10.1109/tia.2011.2168593.
100. Turnbull, F.G. Selected harmonic reduction in static D-C—A-C inverters. *IEEE Trans. Commun. Electron.* **2013**, *83*, 374–378. https://doi.org/10.1109/tcome.1964.6541241.

101. Li, L.; Czarkowski, D.; Liu, Y.; Pillay, P. Multilevel selective harmonic elimination PWM technique in series-connected voltage inverters. *IEEE Trans. Ind. Appl.* **2000**, *36*, 160–170. https://doi.org/10.1109/28.821811.
102. Dahidah, M.S.A.; Konstantinou, G.; Agelidis, V.G. A Review of Multilevel Selective Harmonic Elimination PWM: Formulations, Solving Algorithms, Implementation and Applications. *IEEE Trans. Power Electron.* **2015**, *30*, 4091–4106. https://doi.org/10.1109/tpel.2014.2355226.
103. Patel, H.S.; Hoft, R.G. Generalized Techniques of Harmonic Elimination and Voltage Control in Thyristor Inverters. *EEE Trans. Ind. Appl.* **1973**, *3*, 666–673.
104. Siddique, M.D.; Mekhilef, S.; Padmanaban, S.; Memon, M.A.; Kumar, C. Single-Phase Step-Up Switched-Capacitor-Based Multilevel Inverter Topology With SHEPWM. *IEEE Trans. Ind. Appl.* **2021**, *57*, 3107–3119. https://doi.org/10.1109/tia.2020.3002182.
105. Rodriguez, J.; Moran, L.; Correa, P.; Silva, C. A vector control technique for medium-voltage multilevel inverters. *IEEE Trans. Ind. Electron.* **2002**, *49*, 882–888. https://doi.org/10.1109/tie.2002.801235.
106. Kouro, S.; Bernal, R.; Silva, C.; Rodriguez, J.; Pontt, J. High performance torque and flux control for multilevel inverter fed induction motors. *IEEE Trans. Power Electron.* **2006**, *22*, 805–810. https://doi.org/10.1109/iecon.2006.347906.
107. Banaei, M.R.; Oskouei, A.B.; Dehghanzadeh, A. Extended switching algorithms based space vector control for five-level quasi-*Z* -source inverter with coupled inductors. *IET Power Electron.* **2014**, *7*, 1509–1518. https://doi.org/10.1049/iet-pel.2013.0499.
108. Rony, Z.R.; Das, S.C.; Khan, Z.R. Space Vector Modulated PWM Generation for Motor Control Systems. In Proceedings of the 2018 10th International Conference on Electrical and Computer Engineering (ICECE), Dhaka, Bangladesh, 20–22 December 2018; pp. 149–152. https://doi.org/10.1109/icece.2018.8636720.
109. Qin, S.J.; Badgwell, T.A. An Overview of Industrial Model Predictive Control Technology. *Control Eng. Pract.* **2003**, *11*, 733–764.
110. Papafotiou, G.A.; Demetriades, G.D.; Agelidis, V.G. Technology Readiness Assessment of Model Predictive Control in Medium- and High-Voltage Power Electronics. *IEEE Trans. Ind. Electron.* **2016**, *63*, 5807–5815. https://doi.org/10.1109/tie.2016.2521350.
111. Dekka, A.; Wu, B.; Yaramasu, V.; Fuentes, R.L.; Zargari, N.R. Model Predictive Control of High-Power Modular Multilevel Converters—An Overview. *IEEE J. Emerg. Sel. Top. Power Electron.* **2019**, *7*, 168–183. https://doi.org/10.1109/jestpe.2018.2880137.
112. Wang, Z.J.; Chinthavali, M.; Campbell, S.L.; Wu, T.; Ozpineci, B. A 50-kW Air-Cooled SiC Inverter With 3-D Printing Enabled Power Module Packaging Structure and Genetic Algorithm Optimized Heatsinks. *IEEE Trans. Ind. Appl.* **2019**, *55*, 6256–6265. https://doi.org/10.1109/tia.2019.2938471.
113. Suryanarayana, S.; Ind, P.; Sci, A.; Hill, M. The transistor, a semi-conductor triode. *Phys. Rev.* **1948**, *74*, 230–231.
114. Rajendran, G.; Vaithilingam, C.A.; Naidu, K.; Prakash, K.S.; Ahmed, R. Hard Switching Characteristics of SiC and GaN Devices for Future Electric Vehicle Charging Stations. *MATEC Web Conf.* **2021**, *335*, 02007. https://doi.org/10.1051/matecconf/202133502007.
115. Gamand, F.; Li, M.D.; Gaquière, C.; Algan, A.; Hemts, G. A 10-MHz GaN HEMT DC/DC Boost Converter for Power Amplifier Applications. *IEEE Trans. Circuits Syst. II Express Briefs* **2012**, *59*, 776–779.
116. Transistors, J. The_theory_of_p-N_junctions_in_semiconductors_and_p-N_junction_transistors. *Bell Syst. Tech. J.* **1948**, *28*, 435–489.
117. Shenai, K.; Scott, R.; Baliga, B. Optimum semiconductors for high-power electronics. *IEEE Trans. Electron Devices* **1989**, *36*, 1811–1823. https://doi.org/10.1109/16.34247.
118. Roccaforte, F.; Fiorenza, P.; Greco, G.; Nigro, R.L.; Giannazzo, F.; Iucolano, F.; Saggio, M. Microelectronic Engineering Emerging trends in wide band gap semiconductors (SiC and GaN) technology for power devices. *Microelectron. Eng.* **2017**, *187–188*, 66–77. https://doi.org/10.1016/j.mee.2017.11.021.
119. Millan, J.; Godignon, P. Wide Band Gap power semiconductor devices. In Proceedings of the 2013 Spanish Conference on Electron Devices, Valladolid, Spain, 12–14 February 2013; pp. 293–296. https://doi.org/10.1109/cde.2013.6481400.
120. Zhang, B.; Wang, S. A Survey of EMI Research in Power Electronics Systems with Wide-Bandgap Semiconductor Devices. *IEEE J. Emerg. Sel. Top. Power Electron.* **2020**, *8*, 626–643. https://doi.org/10.1109/jestpe.2019.2953730.
121. Nasr Esfahani, F.; Darwish, A.; Williams, B.W. Power Converter Topologies for Grid-Tied Solar Comprehensive Review. *Energies* **2022**, *15*, 9172.
122. Sharma, A.; Lee, S.J.; Jang, Y.J.; Jung, J.P. SiC based Technology for High Power Electronics and Packaging Applications. *J. Microelectron. Packag. Soc.* **2014**, *21*, 71–78. https://doi.org/10.6117/kmeps.2014.21.2.071.
123. Darwish, A.; Abdelsalam, A.; Massoud, A.; Ahmed, S. Single phase grid connected current source inverter: Mitigation of oscillating power effect on the grid current. In Proceedings of the IET Conference on Renewable Power Generation (RPG 2011), Edinburgh, 6–8 September 2011. https://doi.org/10.1049/cp.2011.0193.
124. Siergiej, R.; Clarke, R.; Sriram, S.; Agarwal, A.; Bojko, R.; Morse, A.; Balakrishna, V.; MacMillan, M.; Burk, J.A.; Brandt, C. Advances in SiC materials and devices: An industrial point of view. *Mater. Sci. Eng. B* **1999**, *61–62*, 9–17. https://doi.org/10.1016/s0921-5107(98)00438-3.
125. Yaramasu, V.; Wu, B.; Sen, P.C.; Kouro, S.; Narimani, M. High-power wind energy conversion systems: State-of-the-art and emerging technologies. *Proc. IEEE* **2015**, *103*, 740–788.
126. Lee, H.; Smet, V.; Tummala, R.; Fellow, L. A Review of SiC Power Module Packaging Technologies: Challenges, Advances, and Emerging Issues. *IEEE J. Emerg. Sel. Top. Power Electron.* **2020**, *8*, 239–255.
127. Wang, F.; Zhang, Z.; Ericsen, T.; Raju, R.; Burgos, R.; Boroyevich, D. Advances in Power Conversion and Drives for Shipboard Systems. *Proc. IEEE* **2015**, *103*, 2285–2311. https://doi.org/10.1109/jproc.2015.2495331.

128. Ji, S.; Zhang, Z.; Wang, F. Overview of high voltage sic power semiconductor devices: Development and application. *CES Trans. Electr. Mach. Syst.* **2017**, *1*, 254–264. https://doi.org/10.23919/tems.2017.8086104.
129. Hornberger, J.; Lostetter, A.B.; Olejniczak, K.J.; McNutt, T.; Lal, S.M.; Mantooth, A. Silicon-carbide (SiC) semiconductor power electronics for extreme high-temperature environments. In Proceedings of the IEEE Aerospace Conference Proceedings, Big Sky, MT, USA, 6–13 March 2004; pp. 2538–2555. https://doi.org/10.1109/aero.2004.1368048.
130. Baliga, B. Power semiconductor device figure of merit for high-frequency applications. *IEEE Electron Device Lett.* **1989**, *10*, 455–457. https://doi.org/10.1109/55.43098.
131. Mantooth, H.A.; Glover, M.D.; Shepherd, P. Wide Bandgap Technologies and Their Implications on Miniaturizing Power Electronic Systems. *IEEE J. Emerg. Sel. Top. Power Electron.* **2014**, *2*, 374–385. https://doi.org/10.1109/jestpe.2014.2313511.
132. Shenoy, J.N.; Member, S.; Cooper, J.A.; Melloch, M.R.; Member, S. High-Voltage Double-Implanted Power MOSFET' s in 6H-SiC. *IEEE Electron Device Lett.* **1997**, *18*, 93–95.
133. Agarwal, A.K.; Casady, J.B.; Rowland, L.B.; Valek, W.F.; White, M.H.; Brandt, C.D. 1.1 KV 4H-SiC Power UMOSFET's. *IEEE Electron Device Lett.* **1997**, *18*, 586–588.
134. Odesanya, K.O.; Ahmad, R.; Andriyana, A.; Bingol, S.; Wong, Y.H. Review—Gate Oxide Thin Films Based on Silicon Carbide. *ECS J. Solid State Sci. Technol.* **2022**, *11*, 083004. https://doi.org/10.1149/2162-8777/ac84ff.
135. Power, B.; Phase, S.; Yin, X.; Shuai, Z.; Member, S.; Shen, Z.J. A New PFC Design With Interleaved MHz-Frequency GaN Auxiliary Active Filter Phase and Low-Frequency. *IEEE J. Emerg. Sel. Top. Power Electron.* **2020**, *8*, 557–566.
136. Chen, P.-C.; Miao, W.-C.; Ahmed, T.; Pan, Y.-Y.; Lin, C.-L.; Chen, S.-C.; Kuo, H.-C.; Tsui, B.-Y.; Lien, D.-H. Defect Inspection Techniques in SiC. *Nanoscale Res. Lett.* **2022**, *17*, 1–17. https://doi.org/10.1186/s11671-022-03672-w.
137. Kimoto, T.; Niwa, H.; Kaji, N.; Kobayashi, T.; Zhao, Y.; Mori, S.; Aketa, M. Progress and future challenges of SiC power devices and process technology. In Proceedings of the 2017 IEEE International Electron Devices Meeting (IEDM), San Francisco, CA, USA, 2–6 December 2017; pp. 9.5.1–9.5.4. https://doi.org/10.1109/iedm.2017.8268360.
138. Schuderer, J.; Vemulapati, U.; Traub, F. Packaging SiC power semiconductors—Challenges, technologies and strategies. In Proceedings of the 2014 IEEE Workshop on Wide Bandgap Power Devices and Applications, Knoxville, TN, USA, 13–15 October 2014; pp. 18–23. https://doi.org/10.1109/wipda.2014.6964616.
139. Basler, M.; Reiner, R.; Moench, S.; Benkhelifa, F.; Doring, P.; Waltereit, P.; Quay, R.; Ambacher, O. Building Blocks for GaN Power Integration. *IEEE Access* **2021**, *9*, 163122–163137. https://doi.org/10.1109/access.2021.3132667.
140. Sun, R.; Lai, J.; Chen, W.; Zhang, B. GaN Power Integration for High Frequency and High Efficiency Power Applications: A Review. *IEEE Access* **2020**, *8*, 15529–15542. https://doi.org/10.1109/access.2020.2967027.
141. Wang, F.F.; Zhang, Z. Overview_of_silicon_carbide_technology_Device_converter_system_and_application. *CPSS Trans. Power Electron. Appl.* **2016**, *1*, 13–32.
142. Amano, H.; Baines, Y.; Beam, E.; Borga, M.; Bouchet, T.; Chu, R.; De Santi, C.; De Souza, M.M. The 2018 GaN Power Electronics Roadmap. *J. Phys. D Appl. Physics* **2018**, *51*, 163001.
143. Ding, X.; Zhou, Y.; Cheng, J. A review of gallium nitride power device and its applications in motor drive. *CES Trans. Electr. Mach. Syst.* **2019**, *3*, 54–64. https://doi.org/10.30941/cestems.2019.00008.
144. Jones, E.A.; Wang, F.F.; Costinett, D. Review of Commercial GaN Power Devices and GaN-Based Converter Design Challenges. *IEEE J. Emerg. Sel. Top. Power Electron.* **2016**, *4*, 707–719. https://doi.org/10.1109/jestpe.2016.2582685.
145. Single, D.; Line, C.; Maruska, H.P.; Tietjen, J.J. The preparation and properties of vapor-deposited single-crystal-line GaN. *Appl. Phys. Lett.* **2004**, *329*, 327–329.
146. Emon, A.I.; Hassan, M.U.; Mirza, A.B.; Kaplun, J.; Vala, S.S.; Luo, F. A Review of High-Speed GaN Power Modules: State of the Art, Challenges, and Solutions. *IEEE J. Emerg. Sel. Top. Power Electron.* **2022**, *11*, 2707–2729. https://doi.org/10.1109/jestpe.2022.3232265.
147. Grown, G.H.; Epitaxy, M.B.; Gan, H.; Distribution, T.; Ieee, P.; Eastman, L.; Devices, H.P. Defense Technical Information Center Compilation Part Notice AIGaN/GaN HEMTs Grown by Molecular Beam Epitaxy on Sapphire, SiC, and HVPE GaN Templates. In Proceedings of the IEEE Lester Eastman Conference on High Performance Devices, Newark, DE, USA, 8 August 2002; pp. 126–133.
148. Zhong, Y.; Zhang, J.; Wu, S.; Jia, L.; Yang, X.; Liu, Y.; Zhang, Y.; Sun, Q. A review on the GaN-on-Si power electronic devices. *Fundam. Res.* **2022**, *2*, 462–475. https://doi.org/10.1016/j.fmre.2021.11.028.
149. Otake, H.; Chikamatsu, K.; Yamaguchi, A.; Fujishima, T.; Ohta, H. Vertical GaN-Based Trench Gate Metal Oxide Semiconductor Field-Effect Transistors on GaN Bulk Substrates. *Appl. Phys. Express* **2008**, *1*, 011105. https://doi.org/10.1143/apex.1.011105.
150. Khadar, R.A.; Liu, C.; Zhang, L.; Xiang, P.; Cheng, K.; Matioli, E. 820-V GaN-on-Si Quasi-Vertical p-i-n Diodes. *IEEE Electron Device Lett.* **2018**, *39*, 401–404.
151. Zhang, K.; Mase, S.; Nakamura, K.; Hamada, T.; Egawa, T. Demonstration of fully vertical GaN-on-Si Schottky diode. *Electron. Lett.* **2017**, *53*, 1610–1611. https://doi.org/10.1049/el.2017.3166.
152. Liu, C.; Khadar, R.A.; Matioli, E. GaN-on-Si Quasi-Vertical Power MOSFETs. *IEEE Electron Device Lett.* **2018**, *39*, 71–74.
153. Diodes, S.B. Vertical GaN-on-Si MOSFETs with Monolithically Integrated Freewheeling. *IEEE Electron Device Lett.* **2018**, *39*, 1034–1037.
154. Kaminski, N.; Hilt, O. SiC and GaN devices—wide bandgap is not all the same. *IET Circuits, Devices Syst.* **2014**, *8*, 227–236. https://doi.org/10.1049/iet-cds.2013.0223.

155. Zhao, D.G.; Xu, S.J.; Xie, M.H.; Tong, S.Y.; Yang, H. Stress and its effect on optical properties of GaN epilayers grown on Si(111), 6H-SiC(0001), and *c*-plane sapphire. *Appl. Phys. Lett.* **2003**, *83*, 677–679. https://doi.org/10.1063/1.1592306.
156. Ikeda, N.; Kaya, S.; Li, J.; Sato, Y.; Kato, S.; Yoshida, S. High power AlGaN/GaN HFET with a high breakdown voltage of over 1.8 kV on 4 inch Si substrates and the suppression of current collapse. In Proceedings of the 2008 20th International Symposium on Power Semiconductor Devices and IC's, Orlando, FL, USA, 18–22 May 2008; pp. 287–290. https://doi.org/10.1109/ispsd.2008.4538955.
157. Mizutani, T.; Ohno, Y.; Akita, M.; Kishimoto, S.; Maezawa, K. A study on current collapse in AlGaN/GaN HEMTs induced by bias stress. *IEEE Trans. Electron Devices* **2003**, *50*, 2015–2020. https://doi.org/10.1109/ted.2003.816549.
158. Su, M.; Chen, C.; Rajan, S. Prospects for the application of GaN power devices in hybrid electric vehicle drive systems. *Semicond. Sci. Technol.* **2013**, *28*, 074012. https://doi.org/10.1088/0268-1242/28/7/074012.
159. Moench, S.; Reiner, R.; Waltereit, P.; Meder, D.; Basler, M.; Ambacher, O.; Kallfass, I. Asymmetrical Substrate-Biasing Effects at up to 350 V Operation of Symmetrical Monolithic. In Proceedings of the 2019 IEEE 7th Workshop on Wide Bandgap Power Devices and Applications (WiPDA), Raleigh, NC, USA, 29–31 October 2019; pp. 28–35.
160. Li, X.; Geens, K.; Wellekens, D.; Zhao, M.; Magnani, A.; Amirifar, N.; Bakeroot, B.; You, S.; Fahle, D.; Hahn, H.; et al. Integration of 650 V GaN Power ICs on 200 mm Engineered Substrates. *IEEE Trans. Semicond. Manuf.* **2020**, *33*, 534–538. https://doi.org/10.1109/tsm.2020.3017703.
161. Reiner, R.; Gerrer, T.; Weiss, B.; Waltereit, P.; Moench, S.; Meder, D.; Sinnwell, M.; Dammann, M.; Quay, R.; Ambacher, O. Si-Substrate Removal for AlGaN/GaN Devices on PCB Carriers.In Proceedings of the 2020 32nd International Symposium on Power Semiconductor Devices and ICs (ISPSD), Vienna, Austria, 13–18 September 2020; pp. 286–289.
162. Zheng, Z.; Song, W.; Zhang, L.; Yang, S.; Xu, H.; Wong, R.K.-Y.; Wei, J.; Chen, K.J. Enhancement-Mode GaN p-Channel MOSFETs for Power Integration. In Proceedings of the 2020 32nd International Symposium on Power Semiconductor Devices and ICs (ISPSD), Vienna, Austria, 13–18 September 2020; pp. 525–528. https://doi.org/10.1109/ispsd46842.2020.9170081.
163. Zheng, Z.; Song, W.; Zhang, L.; Yang, S.; Wei, J.; Chen, K.J. Monolithically Integrated GaN Ring Oscillator Based on High-Performance Complementary Logic Inverters. *IEEE Electron Device Lett.* **2021**, *42*, 26–29. https://doi.org/10.1109/led.2020.3039264.
164. Hu, J.; Zhang, Y.; Sun, M.; Piedra, D.; Chowdhury, N.; Palacios, T. Materials and processing issues in vertical GaN power electronics. *Mater. Sci. Semicond. Process.* **2018**, *78*, 75–84. https://doi.org/10.1016/j.mssp.2017.09.033.
165. Zhang, Y.; Sun, M.; Piedra, D.; Hu, J.; Liu, Z.; Lin, Y.; Gao, X.; Shepard, K.; Palacios, T. 1200 V GaN vertical fin power field-effect transistors. In Proceedings of the 2017 IEEE International Electron Devices Meeting (IEDM), San Francisco, CA, USA, 2–6 December 2017; pp. 9.2.1–9.2.4. https://doi.org/10.1109/iedm.2017.8268357.
166. Review, T. Gallium Nitride Vertical Power Devices on Foreign Substrates: A Review and Outlook. *J. Phys. D Appl. Phys.* 2018, 51 273001.
167. Gupta, C.; Pasayat, S.S. Vertical GaN and Vertical Ga_2O_3 Power Transistors: Status and Challenges. *Phys. Status Solidi (Appl. Mater. Sci.)* **2022**, *219*, 2100659. https://doi.org/10.1002/pssa.202100659.
168. Marquardt, R. Modular Multilevel Converters: State of the Art and Future Progress. *IEEE Power Electron. Mag.* **2018**, *5*, 24–31. https://doi.org/10.1109/mpel.2018.2873496.
169. Song, X.; Cairoli, P.; Du, Y.; Antoniazzi, A. A Review of Thyristor Based DC Solid-State Circuit Breakers. *IEEE Open J. Power Electron.* **2021**, *2*, 659–672. https://doi.org/10.1109/ojpel.2021.3134640.
170. Guicharrousse, P.; Ahmed, R.; Wheeler, P.; Zanchetta, P. New approach for comparing Modular Multilevel Converter submodule losses considering IGBT and SiC MOSFET devices. In Proceedings of the IECON 2022—48th Annual Conference of the IEEE Industrial Electronics Society, Brussels, Belgium, 17–20 October 2022; pp. 1–6. https://doi.org/10.1109/iecon49645.2022.9968842.
171. Sun, Y.; Han, L.; Li, B.; Xu, Z.; Zhou, S.; Xu, D. A Hybrid Modular Multilevel Converter Comprising Si Submodules and SiC Submodules with Its Specialized Capacitor Voltage Balancing Strategy. In Proceedings of the 2022 IEEE Transportation Electrification Conference and Expo, Asia-Pacific (ITEC Asia-Pacific), Haining, China, 28–31 October 2022; pp. 1–6. https://doi.org/10.1109/itecasia-pacific56316.2022.9942174.
172. Yin, T.; Lin, L.; Shi, X.; Jing, K. A Si/SiC Hybrid Full-Bridge Submodule for Modular Multilevel Converter With its Control Scheme. *IEEE J. Emerg. Sel. Top. Power Electron.* **2023**, *11*, 712–721. https://doi.org/10.1109/jestpe.2022.3208602.
173. Liu, H.; Zhou, J.; Zhao, T.; Xu, X. Si IGBT and SiC MOSFET Hybrid Switch-Based Solid State Circuit Breaker for DC Applications. In Proceedings of the 2022 IEEE Energy Conversion Congress and Exposition (ECCE), Detroit, MI, USA, 9–13 October 2022; pp. 1–6. https://doi.org/10.1109/ecce50734.2022.9948172.
174. Liu, H.; Zhao, T.; Wu, X. Performance Evaluation of Si/SiC Hybrid Switch-Based Three-Level Active Neutral-Point-Clamped Inverter. *IEEE Open J. Ind. Appl.* **2022**, *3*, 90–103. https://doi.org/10.1109/ojia.2022.3179225.
175. Priya, K.K. Comparison of Efficiency for Synchronous Buck Converter Using Si and WBG Materials. **2022**, *2022*, 9983108. https://doi.org/10.1109/me54704.2022.9983108.
176. Mhiesan, H.; Umuhoza, J.; Mordi, K.; Farnell, C.; Mantooth, H.A. Evaluation of 1.2 kV SiC MOSFETs in multilevel cascaded H-bridge three-phase inverter for medium-voltage grid applications. *Chin. J. Electr. Eng.* **2019**, *5*, 1–13. https://doi.org/10.23919/cjee.2019.000007.
177. Zhang, L.; Zheng, Z.; Lou, X. A review of WBG and Si devices hybrid applications. *Chin. J. Electr. Eng.* **2021**, *7*, 1–20. https://doi.org/10.23919/cjee.2021.000012.
178. Wang, Y.; Chen, M.; Yan, C.; Xu, D. Efficiency Improvement of Grid Inverters With Hybrid Devices. *IEEE Trans. Power Electron.* **2019**, *34*, 7558–7572. https://doi.org/10.1109/tpel.2018.2881115.

179. Duarte, R.R.; Ferreira, G.F.; Costa, M.A.D.; Alonso, J.M. Performance comparison of Si and GaN transistors in a family of synchronous buck converters for LED lighting applications. In Proceedings of the 2016 IEEE Industry Applications Society Annual Meeting, Portland, OR, USA, 2–6 October 2016; pp. 1–7. https://doi.org/10.1109/ias.2016.7731892.
180. Choudhury, A. Present Status of SiC based Power Converters and Gate Drivers—A Review. In Proceedings of the 2018 International Power Electronics Conference (IPEC-Niigata 2018 -ECCE Asia), Niigata, Japan, 20–24 May 2018; pp. 3401–3405. https://doi.org/10.23919/ipec.2018.8507554.
181. Deshpande, A.; Luo, F. Practical Design Considerations for a Si IGBT + SiC MOSFET Hybrid Switch: Parasitic Interconnect Influences, Cost, and Current Ratio Optimization. *IEEE Trans. Power Electron.* **2018**, *34*, 724–737. https://doi.org/10.1109/tpel.2018.2827989.
182. Deshpande, A.; Luo, F. Design of a silicon-WBG hybrid switch. In Proceedings of the 2015 IEEE 3rd Workshop on Wide Bandgap Power Devices and Applications (WiPDA), Blacksburg, VA, USA, 2–4 November 2015; pp. 296–299. https://doi.org/10.1109/wipda.2015.7369319.
183. Liu, G.; Bai, K.H.; McAmmond, M.; Brown, A.; Johnson, P.M.; Lu, J. Critical short-timescale transient processes of a GaN+Si hybrid switching module used in zero-voltage-switching applications. In Proceedings of the 2017 IEEE 5th Workshop on Wide Bandgap Power Devices and Applications (WiPDA), Albuquerque, NM, USA, 30 October–1 November 2017; pp. 93–97. https://doi.org/10.1109/wipda.2017.8170528.
184. Lourenço, L.F.N.; Perez, F.; Iovine, A.; Damm, G.; Monaro, R.M.; Salles, M.B.C. Stability Analysis of Grid-Forming MMC-HVDC Transmission Connected to Legacy Power Systems. *Energies* **2021**, *14*, 8017. https://doi.org/10.3390/en14238017.
185. Shen, Z.J.; Sabui, G.; Miao, Z.; Shuai, Z. Wide-Bandgap Solid-State Circuit Breakers for DC Power Systems: Device and Circuit Considerations. *IEEE Trans. Electron Devices* **2015**, *62*, 294–300. https://doi.org/10.1109/ted.2014.2384204.
186. Camurca, L.; Liserre, M. Mixed Technology Modular Multilevel Converter Cell—A Cost/Efficiency Analysis. In Proceedings of the IECON 2019—45th Annual Conference of the IEEE Industrial Electronics Society, Lisbon, Portugal, 14–17 October 2019; pp. 6127–6132. https://doi.org/10.1109/iecon.2019.8927289.
187. GaN Systems Unveils Annual Power Semiconductor Predictions for 2023|GaN Systems Technology and Market Overview. *GaN Syst. Mag.* Availaible online: https://gansystems.com/newsroom/2023-power-semiconductor-predictions/ (accessed on 1 November 2022).
188. Teo, K.H.; Zhang, Y.; Chowdhury, N.; Rakheja, S.; Ma, R.; Xie, Q.; Yagyu, E.; Yamanaka, K.; Li, K.; Palacios, T. Emerging GaN technologies for power, RF, digital, and quantum computing applications: Recent advances and prospects. *J. Appl. Phys.* **2021**, *130*, 160902. https://doi.org/10.1063/5.0061555.
189. Kumar, A.; Moradpour, M.; Losito, M.; Franke, W.-T.; Ramasamy, S.; Baccoli, R.; Gatto, G. Wide Band Gap Devices and Their Application in Power Electronics. *Energies* **2022**, *15*, 9172. https://doi.org/10.3390/en15239172.
190. Yin, T.; Lin, L.; Xu, C.; Zhu, D.; Jing, K. A Hybrid Modular Multilevel Converter Comprising SiC MOSFET and Si IGBT with Its Specialized Modulation and Voltage Balancing Scheme. *IEEE Trans. Ind. Electron.* **2022**, *69*, 11272–11282. https://doi.org/10.1109/tie.2021.3118372.
191. Ma, C.-T.; Gu, Z.-H. Review of GaN HEMT Applications in Power Converters over 500 W. *Electronics* **2019**, *8*, 1401. https://doi.org/10.3390/electronics8121401.